NTNU

Norwegian University of
Science and Technology

Microfluidics for Biological Studies

A Double Emulsion Platform for Cell
Encapsulation and Analysis

Camilla Østevold

Master of Science in Physics and Mathematics
Submission date: June 2016
Supervisor: Bjørn Torger Stokke, IFY

Norwegian University of Science and Technology
Department of Physics

Preface

This work is a Master's thesis in TFY4910 Biophysics at the Norwegian University of Science and Technology (NTNU) as a part of the study program *Master of Science in Biophysics and Medical Technology*, and was carried out spring 2016 at the NTNU Microfluidics Group under supervision of Professor Bjørn Torger Stokke. The thesis is based on the work "Microfluidics for synthesis of double emulsions – optimization of 3D geometries for spatially controlled surface treatment" carried out fall 2015 by the same author, as a part of the course TFY4500 Biophysics, Project Thesis. Fabrication of microfluidic devices was done at the NTNU Nanolab, which is a part of The Norwegian Micro- and Nanofabrication Facility (NorFab). Microbiological samples were kindly provided by Rahmi Lale (Department of Biotechnology) and Gunvor Røkke (Department of Biotechnology, Department of Biology). Professor Esther Amstad and Gianluca Etienne (Soft Materials Laboratory, École polytechnique fédérale de Lausanne, Switzerland) are thanked for the generous donation of surfactant used in this project. I would also like to thank Sofie Snipstad for her helpful guidance with the flow cytometry analysis, Kristine Østevold for her artistic contribution, and Karl Gullik Nakken and his MacBook Pro for tech support. Lastly, I would like to express my gratitude to the entire NTNU Microfluidics group, especially my co-supervisor Armend Gazmeno Håti for his invaluable support and assistance throughout my final year at NTNU.

Trondheim, 2016-06-15

Camilla Østevold

Abstract

Encapsulation of biological material in small, confined volumes has enabled the study of individual cells, revealing valuable and detailed information on cellular processes and behavior unavailable in traditional bulk studies. This work presents a double emulsion platform for the encapsulation and analysis of biological material. Double emulsions were synthesized in 3D microfluidic PDMS devices and immobilized on PDMS microarrays for imaging purposes. The effect of flow rates on droplet sizes and amount of double emulsion cores was explored, however, no definite relationship was determined due to variations in the system. The origin of these variations was probably device alignment, surface treatment, the tubing of the syringe pump system, or a combination thereof. The fluorosurfactant provided by SMaL at EPFL rendered the double emulsions stable with regards to coalescence, temperature variations, and shear forces exerted by the carrier fluid. The greatest challenge in terms of stability appeared to be osmotic pressure differences between the double emulsion cores and the surrounding medium. However, it is likely that this obstacle can be overcome by a thorough measurement of the osmolarities of the inner and outer phases and subsequent balancing of possible differences by the addition of sucrose. Double emulsion cores containing 0.60%, high G-content alginate (M_w = 275 kDa) and chelated calcium ions were gelated for the synthesis of spherical, micron-sized hydrogels. Two different internal gelation methods were investigated; pH-triggered gelation and a novel gelation method recently established at NTNU termed CLEX. Both successfully synthesized hydrogels, however, CLEX is favorable for biological systems as it occurs at neutral pH-values. Additionally, a device with two inner phase inlets was applied for gelation of alginate cores by CLEX. This device introduces the possibility of on-chip mixing of double emulsion cargo, which may be utilized for studies of cellular processes such as bacterial conjugation. *Pseudomonas Putida* and *Chlamydomonas reinhardtii* were encapsulated on-chip with high throughput, resulting in compartmentalization of single or few cells in suitable microenvironments. Three different encapsulation media were tested for their compatibility with a droplet-based microfluidic system and living material; 20% PEG, 0.60% and 0.15% alginate. The latter provided a viable and healthy microenvironment for cell growth. Double emulsions with 0.15% alginate cores and the microarray thus represent a suitable platform for microbiological studies if the osmotic instability issue is resolved.

Sammendrag

Innkapsling av biologisk materiale i små, begrensede volum har muliggjort studier av den individuelle celle på et betraktelig mer detaljert nivå enn hva som har vært tilgjengelig i tradisjonelle bulkstudier. Dette arbeidet fremstiller en plattform for innkapsling og analyse av biologisk materiale basert på doble emulsjoner. Doble emulsjoner ble fremstilt i 3D mikrofluidtekniske PDMS-enheter og immobilisert på PDMS mikromatriser for avbildning. Effekten av strømningsrater på dråpestørrelse og antallet kjerner i de doble emulsjonene ble utforsket, som følge av variasjoner i systemet ble det derimot ikke fastsatt et klart forhold mellom disse. Slike variasjoner oppstår mest sannsynlig på grunn av justering av PDMS-enhetene, overflatebehandling, feil i injeksjonsslangene, eller en kombinasjon derav. Fluorosurfaktanten fra SMaL ved EPFL stabiliserte de doble emulsjonene med hensyn til koalesens, temperaturvariasjoner og skjærkrefter som utøves av transportvæsken. Den største utfordringen for stabilitet viste seg å være forskjeller i osmotisk trykk mellom kjernen av de doble emulsjonene og den omgivende væsken. Denne hindringen kan imidlertid mest sannsynlig overkommes ved nøyaktige målinger av osmolaritetene til de aktuelle væsker og en påfølgende balansering av eventuelle forskjeller ved tilsetting av sukrose. Kjerner bestående av 0.60%, høyt G-innhold alginat (M_w = 275 kDa) og kelaterte ioner ble gellet for fremstilling av sfæriske, mikrohydrogeller. To ulike metoder for intern gelling ble undersøkt; gelling ved endring av pH, og en ny metode nylig utviklet ved NTNU kalt CLEX. Begge metoder førte til vellykket fremstilling av hydrogeller, likevel er CLEX å foretrekke for biologiske systemer ettersom denne metoden utføres ved nøytrale pH-verdier. I tillegg ble en PDMS-enhet med to innløp for den indre fase brukt for gelling av alginatkjerner ved bruk av CLEX. Denne enheten introduserer muligheten for on-chip miksing av ulike kjernekomponenter, hvilket kan brukes for studier av celleprosesser som blant annet bakteriell konjugasjon. *Pseudomonas Putida* and *Chlamydomonas reinhardtii* ble innkapslet on-chip med høy gjennomstrømning i doble emulsjoner. Tre ulike innkapslingsmedier ble testet; 20% PEG, 0.60% og 0.15% alginat. Den sistnevnte representerte et levedyktig og sunt mikromiljø for cellevekst. Doble emulsjoner med 0.15% alginatkjerner representerer sammen med mikromatrisen en passende plattform for mikrobiologiske studier hvis problemene knyttet til osmotiske trykkforskjeller løses.

Contents

Chapter 1

Introduction

For more than a 100 years, techniques such as plate counting and light microscopy have provided scientists with valuable information on the features and activities of individual microbial cells[1]. As technology has advanced, further insight into cellular processes has been gained through methods such as in situ hybridization and polymerase chain reaction (PCR), as well as improved computational and imaging techniques. Access to information on a molecular level is a crucial step on the road to understanding cellular phenomena such as gene transfer, intercellular communication and cell death.

The excessive use of various antibacterial drugs over the last decades has resulted in the emergence of multiresistant bacteria that pose a serious threat to public health worldwide. If not dealt with, antibiotic resistance in bacteria that cause infections such as tuberculosis, pneumonia or gonorrhea will not only increase the cost of health care and impede the control of bacterial proliferation, but also greatly increase the risk of death for infected patients[2]. Resistance to main classes of antimicrobial agents are efficiently spread through the transfer of plasmids that encode resistance genes. Plasmid transfer occurs through bacterial conjugation or transformation[3], the detailed mechanisms of which still remain unclear[4]. Bacterial gene transfer is thus one of many important cellular processes yet to be revealed through further studies, where in particular single-cell approaches are expected to be important.

Although technology has already come a long way, new methods for single-cell studies are ever in demand. This work aims to establish a platform for single cell studies and analysis

using biophysical microtechniques. More precisely, a microfluidic strategy for cell encapsulation is tested, where immobilized double emulsions synthesized in 3D microfluidic devices serve as cell microcapsules. The properties of the double emulsions are explored to determine the overall suitability of the system as a platform for microbiological studies. Additionally, the the possibility of hydrogel synthesis is examined and the prospect of double emulsion as cell-laden hydrogel precursors is discussed.

Chapter 2

Background

Cellular processes such as differentiation, gene expression, chemical communication and gene transfer have traditionally been studied at the population level. However, bulk-scale measurements on a population of cells only report average values for the population, and lack information on a single cell level[1]. The individual microorganisms of a clonal population may differ widely from each other in terms of genetic composition, physiology, biochemistry or behavior, and each cell experiences a unique microenvironment that influences their development and function[5]. Single-cell observation and analysis are therefore of great importance in microbiological research, as this detailed level of microbial observation can provide valuable information on phenomena such as antibiotic resistance and mechanisms of pathogenesis, among others. Techniques such as flow cytometry and fluorescence activated cell sorting (FACS) have commonly been used for single-cell analysis.

Single cell analysis functionality is greatly enhanced by encapsulation in small, confined volumes. Compartmentalization isolates the cell with any reagents or secreted molecules that might be present, and maintains the specific biological microenvironment. Encapsulation also protects sensitive cells from shear damage in suspension culture[6]. Cell capsules must meet several important criteria for successful cell survival, growth and shielding, which may depend on the specific application. However, general criteria for a healthy cell environment include non-toxicity and permeability to oxygen, incoming nutrients, and outgoing toxic metabolites[7]. Furthermore, cell capsules should be mechanically strong and thermally stable[8]. Different cell encapsulation strategies have been explored, such as encapsulation in porous silica gel and alumina matrices using a sol-gel process[8][9] and encapsula-

tion in nano-organized polyelectrolyte shells by alternate adsorption of oppositely charged species[10]. Polymer-based encapsulation, another popular encapsulation format, is based on confining cells in hydrogel microbeads. Cell-laden hydrogels show promising potential in fields such as tissue engineering, regenerative medicine, cell-based drug delivery[11], treatment of hormone or protein deficient diseases, and cancer therapy[12]. Alginate is particularly suitable as cell encapsulation medium due to its biocompatibility, biodegradability, similarities to the natural extracellular matrix, and ease of gelation[13]. Additionally, confinement in water-in-oil emulsions synthesized in a droplet-based microfluidic system using biocompatible and inert fluids has turned out as a successful encapsulation strategy that maintains cell viability and healthy metabolism[14]. Modification of the oil-water interface in a emulsion-based encapsulation system enables selective control of diffusion between the droplet and its environment, or between individual droplets. Surfactants in either of the phases play an essential part in droplet-based microfluidics by enhancing droplet stability and mechanical strength, as well as in the process of molecular exchange between droplets[15]. Here, hydrogel synthesis and cell encapsulation using droplet microfluidics will be discussed.

Droplet-based microfluidics has indisputably become the most common strategy for cell encapsulation[5][14], as microfluidic devices offer automation and high-throughput while operating at low volumes of consumables[16]. Micron-sized, uniform particles are synthesized by injecting immiscible fluids in microchannels with geometries that enable viscous and surface tension forces to cause the formation of a dispersed two-phase flow, usually water-in-oil single emulsions[17]. The advantages of droplet-based microfluidics has enabled the application of emulsion capsules in high-throughput drug screening[18], rare cell detection[19], directed enzyme evolution[20], discovery of promiscuous enzymes[21], bacterial communication studies[22], and encapsulation, incubation, and analysis of single cells[14], to mention some. Furthermore, droplet-based microfluidic systems are well-suited for the synthesis of hydrogels as they provide a high degree of uniformity and regularity in terms of shape and size[11] compared to gravitational[7] or electrostatic extrusion[23][24]. Other approaches to hydrogel synthesis such as photolithography, micromolding and centrifuge-based drop makers also provide size and shape control, but rely on processing techniques that result in low throughput compared to microfluidic systems[25]. Different gelation tech-

niques have been applied for synthesis of alginate hydrogels in microfluidic channels. Internal gelation is generally preferred, as it gives better control of hydrogel size, shape and homogeneity than external gelation methods. Gelation can be brought about by mixing the alginate with an insoluble calcium salt and triggering release of calcium ions by lowering the pH[11].

Single water-in-oil emulsions have several limitations that restrict their application as microcapsules for living material. The oil carrier fluid does not allow continuous supply of nutrient or inducer molecules, and is incompatible with aqueous phase-based analysis such as flow cytometry[26]. However, these challenges can be overcome by adding an outer aqueous phase to the microdroplet system, creating water-in-oil-in-water (WOW) double emulsions (Figure 2.1). WOW double emulsions consist of oil emulsion drops with aqueous cores, where the oil phase serves as a layer separating the core from the aqueous carrier fluid[27]. Furthermore, the oil shell functions as a semi-permeable membrane, enabling selective transport both in and out of the capsule[26]. Compared to single emulsions, double emulsions are more difficult to form and stabilize as more phases and interfaces are involved in the emulsification process[27]. However, fabrication of double emulsions can be achieved with 3D microfluidic devices that provide a two-step droplet break-up and 3D geometries which assure that the dispersed phase is surrounded by the continuous phase[28]. Additionally, careful hydrophilic and hydrophobic surface treatment of the channel walls is often required for controllable and reliable synthesis of double emulsions. Double emulsions have been proven as useful assays for cell cultivation[26], *in vitro* green fluorescence protein expression[29] and bacterial biofilm growth[30], among others. Moreover, double emulsions may also be applied for the synthesis of uniform hydrogels. Compared to single emulsion-based techniques, the use of WOW double emulsion as hydrogel precursors reduces the need for organic component, which is favorable as the oil environment decreases the viability of cells laden in the microgels[25][31].

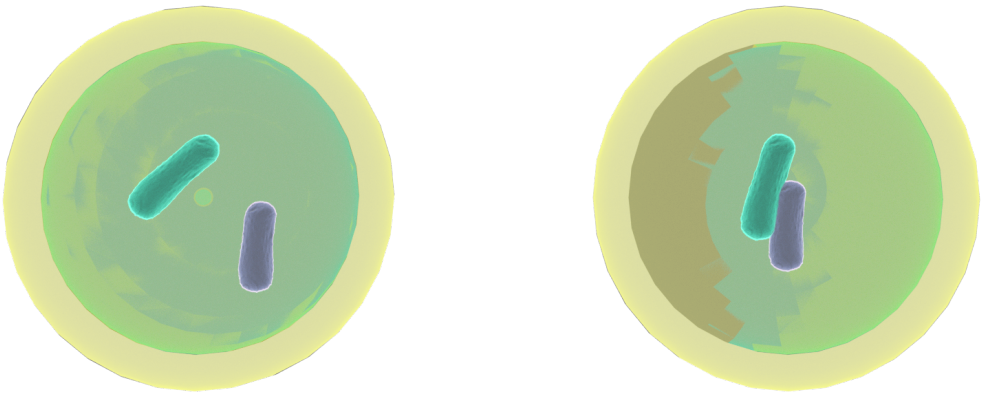

Figure 2.1: Visualization of bacteria encapsulated in double emulsions with aqueous cores and oil shells. Courtesy of the NTNU Microfluidics group.

Chapter 3

Theory

3.1 Microfluidics

Describing a flow situation

In a given flow situation, the determination of the properties of the fluid as a function of position and time is to be concidered to be the solution of the problem. Foremost among the properties of a flow is the velocity field $\mathbf{V}(x, y, z, t)$, as most other properties follow directly from the velocity field. In general, velocity is a vector function of position and time and thus has three components u, v and w, each a scalar field in itself:

$$V(x, y, z, t) = \mathbf{i}u(x, y, z, t) + \mathbf{j}v(x, y, z, t) + \mathbf{k}w(x, y, z, t). \tag{3.1}$$

The velocity field is highly dependent on the thermodynamic properties of the fluid, such as pressure p, density ρ and temperature T[32].

A mathematical description of viscous fluid motion can be given by a set of differential equations based on the conservation of mass, momentum and energy. An analysis of linear momentum conservation yields the basic differential momentum equation for fluid motion:

$$f_{\boldsymbol{body}} - \nabla p + \nabla \bullet \tau_{ij} = \rho \frac{d\mathbf{V}}{dt}, \tag{3.2}$$

where f_{body} is the body force, p is the pressure force,τ_{ij} is the viscous stress tensor, ρ is the density, and $\frac{d\mathbf{V}}{dt}$ is the acceleration. Body forces refer to gravitational forces, among

others[33]. The derivation is omitted here, but the devoted reader is directed to read Frank M. White's *Fluid Mechanics*, 6th edition, pages 234-239[32] for an elaboration on the subject. For fluids where the viscosity coefficients in the viscous stress tensor τ_{ij} can be considered as constants, the viscous stress component can be represented by the fluid's dynamic viscosity μ. The dynamic viscosity is a quantitative measure of a fluid's resistance to flow, and is defined as the ratio of shear stress τ to shear rate $\dot{\gamma}$:

$$\mu = \frac{\tau}{\dot{\gamma}}. \tag{3.3}$$

The SI unit of μ is Pascal-seconds, Pa s. Fluids that follow the relationship described by Equation 3.3 are called newtonian fluids[32], for which the three-dimensional differential momentum equations become the Navier-Stokes equations. These are are second-order nonlinear partial differential equations that only have a limited number of known analytic solutions. In cases where the flow velocities are much smaller than the velocity of pressure waves in the liquid, the fluid can be treated as incompressible[33]. For an incompressible, newtonian fluid, the Navier-Stokes equations simplify to

$$\rho \frac{d\mathbf{V}}{dt} = f_{\boldsymbol{body}} - \nabla p + \mu \nabla^2 \mathbf{V}, \tag{3.4}$$

written in their compact form. Equation 3.4 can be solved for a variety of interesting flow problems where certain simplifications can be made. For the liquid-solid interface the no-slip boundary condition applies, which means that the velocity of the liquid equals the velocity of the wall at the interface. Finally, for stationary systems ($d\mathbf{V}/dt = 0$) where body forces can be ignored, the Navier-Stokes equation is reduced to the Stokes equation[32]:

$$\nabla p = \mu \nabla^2 \mathbf{V}. \tag{3.5}$$

Solving the Stokes equation usually involves writing it in its non-dimensional form, which can greatly simplify the problem if scaling factors are carefully chosen for a given system. One such scaling factor is the dimensionless Reynolds number, which is commonly introduced as a scaling factor for simplification of Equation 3.4. It is given by

$$\mathrm{Re} = \frac{\rho V L}{\mu}, \tag{3.6}$$

where V and L are characteristic velocity and length scale of the flow. Low Reynolds numbers (Re << 1) are associated with the laminar regime, where viscous forces dominate inertial forces[32]. For a laminar regime the body forces in Equation 3.4 are neglected, and if the flow is stationary, Equation 3.5 applies.

Flow in long microchannels

Given the small dimensions of microchannels, microfluidic flows experience low Reynolds numbers. Microfluidics thus typically operate in laminar regimes which allows highly controlled deterministic fluid flow. Furthermore, operating within a laminar flow regime indicates that viscous stress forces will be important in flow events such as droplet formation in microfluidic systems[33]. For pressure driven, laminar flows of incompressible fluids in a straight circular pipe of radius R, an analytical solution of Equation 3.5 exists. The flow is assumed to be fully developed, which implies that the region studied is far enough from the inlet so that the flow is purely axial. A purely axial flow is only directed along the length of the pipe (z-direction in cylindrical coordinates) with no radial motion. Solving the Stokes equation as a function of the distance r from the centerline, with no-slip at the wall ($\nabla \cdot V = 0$) and finite velocity at the centerline as boundary conditions, yields the solution for fully developed Hagen-Poiseuille flow in a circular pipe[32]:

$$v_z(r) = \left(-\frac{dp}{dz}\right)\frac{1}{4\mu}(R^2 - r^2). \tag{3.7}$$

The velocity profile is a paraboloid with a maximum at the centerline, as shown in Figure 3.1.

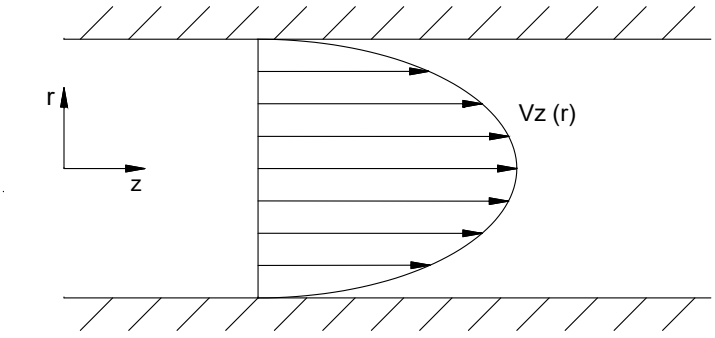

Figure 3.1: The velocity profile of Hagen-Poiseuille flow in a circular pipe[32].

It is reasonable to assume that fluids in a microfluidic system are close to incompressible due to the low velocities realized at this scale[33]. Furthermore, the dimensions in a long microchannel make it reasonable to assume that the flow is fully developed and laminar, such that Equation 3.7 and the flow velocity profile in Figure 3.1 adequately describe the flow situation of newtonian fluids in a microfluidic system of circular channels. For rectangular channels certain approximations must be made to solve the Navier-Stokes equations, as no exact analytic solutions exist. However, the flow profile in a microfluidic system of rectangular channels will resemble that of Figure 3.1.

3.2 Droplet-based microfluidics

Droplet-based microfluidics is a variant of microfluidics based on the formation of droplets driven by viscous drag forces and surface tension in a two-phase microchannel system[34]. The formation of oil droplets in water, or vice versa, is called an emulsion, which is a type of colloidal dispersion where both phases are liquids. In a colloidal system, the surface area to volume ratio is unusually large. The properties of a colloidal dispersion is therefore heavily dependent on the surface properties[35].

Surface tension

In a colloidal system the surface is defined as a phase separation of molecular dimensions[36]. The interface between two liquids (or gases) can be adequately described by the concept of surface tension. Molecules at the surface of one liquid are missing half of their neighbors compared to those deep within the liquid, and thus experience a net force directed towards the bulk. The surface will therefore attempt to decrease its area, and the mechanical effect is that the surface is in tension. The surface tension is defined as force per unit length, and is usually described by the coefficient of surface tension, Υ [$\mathrm{N\,m^{-1}}$]. Another way to quantify surface tension is by regarding it as the origin of a new surface free energy, that is, it takes energy to create a new surface. By this definition Υ is given by

$$\Upsilon = \left(\frac{dG}{dA}\right)_{T,P}, \tag{3.8}$$

and describes the increase in surface free energy (dG) per unit area (dA) at constant temperature T and pressure (P) [$\mathrm{J\,m^{-2}}$][35].

Laplace pressure

As mentioned in the previous section, an interface will always attempt to minimize its area, thus minimizing the total surface free energy. A sphere has the lowest surface to volume ratio of all geometrical shapes, and is therefore the energetically favorable state. This makes the sphere the preferred geometrical shape for emulsions and other types of colloidal dispersions. When a curved surface is in mechanical equilibrium with its surroundings, the pressure on the concave side equals the pressure on the convex side and the opposing pressure that rises from surface tension components. There must accordingly exist a balancing pressure difference ΔP over the interface. This pressure difference is inversely proportional to the radius of the curvature, and is the direct cause of many phenomenons and processes that are characteristic for colloidal systems. It is given by the Young-Laplace equation as a function of the two radii that define the curvature of a given point on the surface and the surface tension coefficient:

$$\Delta p = \Upsilon \left(\frac{1}{R_1} + \frac{1}{R_2} \right). \tag{3.9}$$

The pressure is always larger on the concave side of the interface. For a spherical liquid droplet R_1 equals R_2 (= R), so that Equation 3.9 reduces to

$$\Delta p = \frac{2\Upsilon}{R}. \tag{3.10}$$

Δp, sometimes called the Laplace pressure, is larger for smaller droplets, as indicated by Equation 3.10[35].

Surfactants

Surfactants are surface active agents that have a distinct tendency of adsorbing to interfaces. In doing so, surfactants significantly reduce the surface tension between two phases, even at very low concentrations. This is owed to the amphiphilic nature of surfactants, i.e., they contain both lyophilic and lyophobic groups. Lyophilic groups have an affinity for the continuous phase whereas lyophobic groups will precipitate in the continuous phase. In water the equivalent terms are hydrophilic and hydrophobic groups[35]. When an amphiphilic molecule is dissolved in water, the water molecules will arrange in a structured order around the hydrophobic groups without forming energetically favorable bonds. This results in a de-

crease in the entropy of the system, which increases the Gibbs free energy $G(p,T)$, given by

$$G(p,T) = H - TS, \tag{3.11}$$

where H is the enthalpy, T is temperature and S is the entropy[37]. As a system always strives to lower its free energy, the water molecules will attempt to minimize this effect by pushing the lyophobic groups to the surface. In the case of emulsions, the surfactants thus form a mechanically strong, adsorbed mono-molecular layer around the dispersed phase[35]. Moreover, surfactants may contribute to molecule transport over inherently impervious interfaces by forming bilayers between droplets[15]. Surfactant bilayers are two-layered surfactant sheets with the lyophobic groups pointed towards the center of the sheet. Similar to the lipid bilayers that make up cell membranes, surfactant bilayers are porous to certain molecules[38]. Commercially available surfactants such as oligomeric perfluorinated polyethers (PFPE) are soluble in fluorocarbon oils and may be applied to stabilize emulsions. These do, however, contain functional groups, particularly COOH that may interact with biomolecules such as proteins and DNA. Nonionic biocompatible surfactants have been specially designed to stabilize emulsions systems, usually synthesized by coupling PFPE with a hydrophilic component, typically polyethyleneglycol (PEG)[39]. Others have demonstrated the synthesis of PFPE surfactants with (hydroxymethyl)methyl (Tris)[40] or polyglycerols [41] as a hydrophilic component, although these structures are not yet commercially available. The presence of different cations and anions may lower or raise the cloud point of PEG through dehydration and electrostriction[42]. The cloud point is the temperature above which the polymer chain collapses and precipitates in solution, causing an increase in solution turbidity.

Droplet formation

Mathematically, the break-up of fluid jets is explained by the instability of the Hagen-Poiseuille solution (Equation 3.7) to the Stokes equation (Equation 3.5)[43]. Plateau (low viscosity), and later Rayleigh (viscous flow), showed that a liquid jet subject to surface tension at its free interface develops perturbations on the surface over time, resulting in varying thickness along the length of the jet[44]. Equation 3.10 shows that a local change in the radius of curvature changes the pressure due to surface tension. The perturbations thus cause a local increase

and decrease in pressure which eventually may break the jet up into energetically favorable droplets as the surface tension is decreased[45]. If the column of liquid is surrounded by another immiscible viscous medium, viscous drag may break the continuous flow into discrete fluid elements[44]. The surrounding medium, or the carrier fluid, is commonly referred to as the continuous phase, while the droplet elements are called the dispersed phase[35]. Surfactants play an important part in droplet formation by lowering the surface tension between the two phases (Section 3.2).

3.3 Double emulsions

Double emulsions consist of emulsion drops with smaller droplets inside, usually water-in-oil-in-water (WOW), where the oil phase serves as a layer separating the aqueous core from the aqueous carrier fluid[27]. WOW double emulsions can be synthesized in a double flow focusing device, where water-in-oil droplets or jets are formed at the first junction and oil-in-water droplets at the second junction[46]. A two-step emulsification process can lead to a more polydisperse sample[47]. To avoid this issue, devices have been made where no emulsification occurs at the first junction, instead a laminar two-phase co-flow is formed. A lower continuous phase contact angle, i.e., more extensive outer phase wetting, will result in the dispersed phase being pinched off more easily. Equivalently, high contact angle of the dispersed phase also aids droplet formation[34]. Non-planar 3D-devices further aid droplet formation as the cross-sectional area of the dispersed phase channel is smaller than that of the continuous phase channel, allowing the dispersed phase to be completely engulfed by the continuous phase at the junction[48]. An illustration of a 3D geometry double emulsion synthesis device is shown in Figure 3.2.

The stability of double emulsions

Double emulsions are considered thermodynamically stable if their lifetime is long enough for the governing practical purpose they are made for. In any colloidal system, Brownian motion and forced hydrodynamic motion will both lead to collisions between the dispersed particles. If a collision brings two particles close enough, the attractive forces will be larger than the repulsive forces and the particles will likely coalesce. In the case of emulsions, particle collision may cause a fusion of droplets which includes a strong reduction of the total

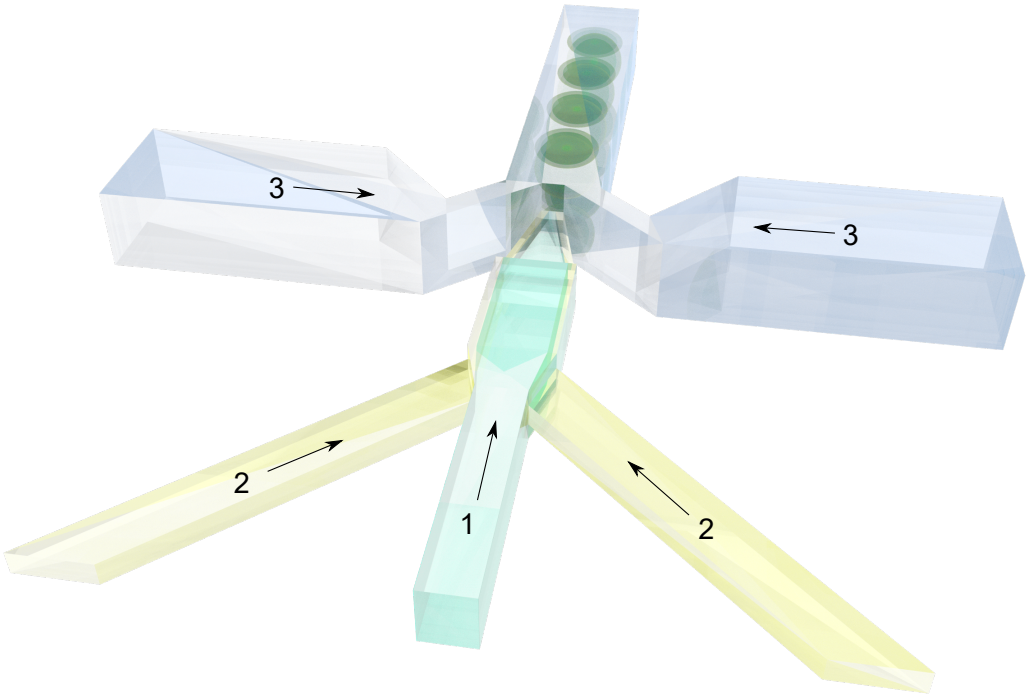

Figure 3.2: Illustration of a 3D double emulsion device. The inner aqueous phase (1) and oil phase (2) meet at the upper junction and form a laminar, two-phase co-flow. Droplet formation occurs as the co-flow passes through a nozzle and enters the continuous phase channel (3). WOW-droplet formation is aided by the wetting properties in the nozzle and junction areas and the presence of surfactants (Section 3.2). Courtesy of the NTNU Microfluidics group.

particle surface area[35]. As mentioned in Section 3.2, surfactants stabilize the droplet interface by balancing the driving force towards coalescence, mainly by steric repulsion of the surfactant molecules. Another process inhibiting coalescence is the so-called Marangoni effect in the presence of surfactants (Figure 3.3). As the droplet moves through the viscous medium, the surfactant distribution is non-uniform, with an excess at the rear end of the droplet. This creates a surfactant gradient in the direction of lower surfactant concentration, which gives rise to a Marangoni stress opposing the flow. For droplet collision to occur, the layer of the continuous phase that separates the droplets has to be drained. However, this drainage is delayed by the Marangoni stress, and the emulsions are therefore stabilized against coalescence. The presence of surfactants also hinder the rupture of the double emulsions when experiencing high shear stress exerted by the carrier fluid[15].

In addition to coalescence and shear stress, osmotic pressure differences between the inner and outer aqueous phases must also be accounted for to maintain double emulsion stability. The osmotic pressure is the opposing pressure needed to hinder fluid flow in an osmotic

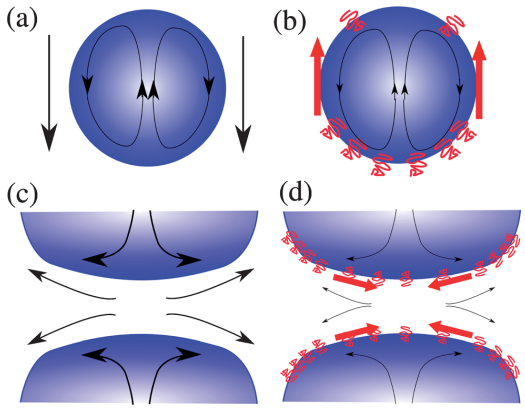

Figure 3.3: The Marangoni effect. A: A droplet in motion in the absence of surfactants. The black arrows indicate the motion of the surrounding fluid. B: Surfactants present in the solution concentrate at the rear end of the droplet, causing a surfactant gradient (red arrows). C: As two droplets approach each other, the layer of the continuous phase that separates the droplets has to be drained for collision to occur. D: In the presence of surfactants, the drainage of the continuous phase layer is delayed by the surfactant gradients that rise due to the drainage itself. Figure from Baret, *Lab On a Chip*, 2012[15].

process, and is related to the molar concentration of present solutes[35]. The origin of an osmotic process is a difference in chemical potential over a semi-permeable membrane which renders the system in a non-equilibrium situation. The resulting potential gradient causes diffusion of molecules over the membrane towards lower chemical potential in order to restore equilibrium in the system.

Double emulsion core material

Double emulsion constituents are chosen not only for their biocompatibility, but also for their droplet formation abilities in a microfluidic system. As mentioned in Section 3.2, viscous drag forces play an important part therein and the fluids must therefore exhibit viscosities suitable for microfluidic assisted droplet break-up. Solutions of about 10% polyvinyl alcohol (PVA) are suitable as carrier fluid for the formation of oil emulsions in a water phase[34]. A perfluorinated oil, HFE7500, is suitable for the oil phase with a viscosity about 0.8 times that of water at 20 °C[49][50]. Two possibilites for the inner phase fluid are described in the subsequent sections; aqueous PEG and alginate.

Polyethylene glycol

Polyethylene glycol is an ethylene oxide polymer soluble in water and most organic solvents. PEG is commonly used in droplet microfluidics due to its suitable viscosity, availability[51][34],

and reported non-toxicity (PEG is commonly used in pharmaceuticals and food additives[52]). However, studies have shown that PEG causes a loss of viability in certain strains of bacteria[53][54][55].

Alginate

Alginates are a family of anionic polysaccharides produced by algae and some bacteria. All alginates are linear block copolymers containing blocks of β-D-mannuronic acid (Figure 3.4a) and α-L-guluronic acid (Figure 3.4b) residues linked by 1→4 linkages (Figure 3.5). The ratio of β-D-mannuronic acid (M) or α-L-guluronic acid (G) are given by the residue fractions F_M and F_G, respectively. A residue fraction of 0.50 corresponds to 50% presence in the chain, such that F_M + F_G always equals 1[56]. Blocks may contain consecutive M residues (MMMMM), consecutive G residues (GGGGG) or alternating M and G residues (GMGMG). The number of G and M residues, as well as the length of each block, vary depending on the alginate source. Of particular importance is the length and number of consecutive G blocks, as they are believed to play an important part in intermolecular cross-linking with divalent cations to form hydrogels. Various alginate derivatives are largely applied in biomedicine, due to their biocompatibility, low toxicity, relatively low cost and ease of gelation[13].

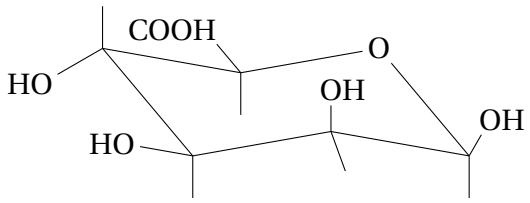

(a) $^4C_1$ chair form of β-D-mannuronic acid (M).

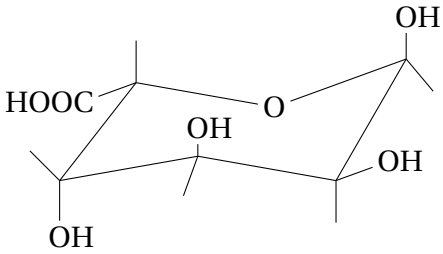

(b) $^1C_4$ chair form of α-L-guluronic acid (G).

Figure 3.4

All blocks of alginates are polyanionic and able to form ionic bonds to di- or multivalent cations. However, repeating G-blocks are additionally able to chelate the metal ions due to the spatial arrangement of the ring and hydroxyl oxygen atoms. This creates so-called junction zones, where two chains of alginate associate as dimers of G-blocks bind to the cation on

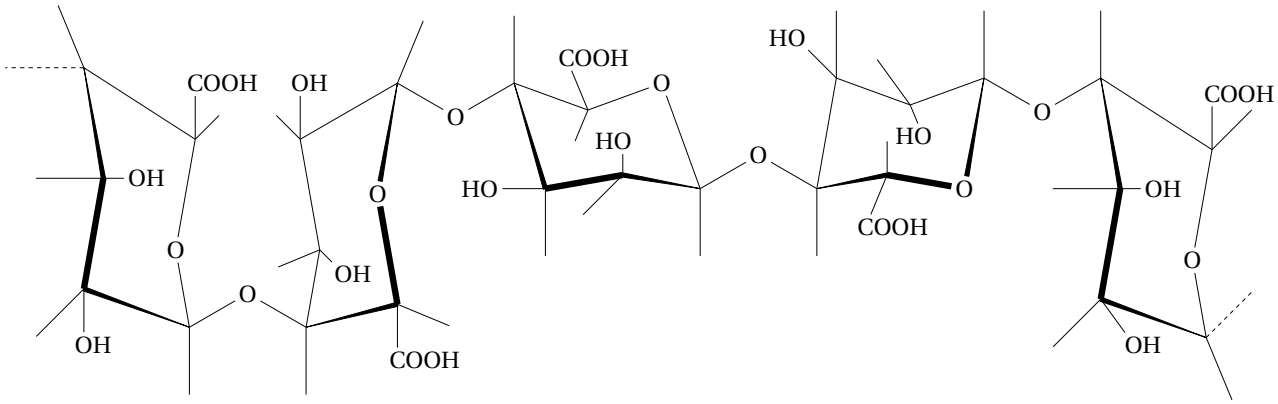

Figure 3.5: 1→4 linked alginate (GGMMG).

both sides. Ionic cross-linking of junction zones is called the egg-box model of gelation[57], illustrated in Figure 3.6. The associated alginate chains form a three-dimensional cross-linked network of hydrophilic polymers with a high water content, also called hydrogels[13]. Gelation can be induced externally or internally, which denotes the method of introducing the metal ions (usually Ca^{2+}). In external gelation metal ions are introduced through the carrier fluid, often after droplet synthesis by extrution of alginate droplets into a solution of calcium salt, resulting in an almost instantaneous cross-linking process. More controlled and microfluidic compatible gelation kinetics can be achieved by internal gelation, as the cross-linking ions are introduced in the alginate solution in an insoluble form before droplet synthesis[58][59]. Gelation is then brought about by changing the conditions of the carrier fluid to trigger the release of calcium ions into solution. Internal gelation yields more homogeneous and permeable gels than external gelation, however, external gelation generally yields a stronger gel for a given amount of cross-linker ions[60]. The cross-linking ions may be contained as a partly insoluble solid salt (e.g. $CaCO_3$) or as a chelate (e.g. Ca-Ethylenediaminetetraacetic acid, CaEDTA). Triggering the release of calcium ions can be done by altering the pH, either by the addition of acid or a hydrolysing agent such as D-glucono-δ-lactone, the latter resulting in a slower release of cross-linking ions than the former[61]. However, introducing solid salts in microchannels might result in clogging over time, and low pH values may be toxic to many types of cells. To resolve this issue, Bassett, Håti, *et al.* devised a more biocompatible internal gelation technique for gelation in microfluidic devices called competitive ligand exchange crosslinking (CLEX) (Bassett, Håti, *et al.*, Submitted May 2016). Here, gelation ions and exchange ions are bound to cation chelators and their relative affinities to chelators versus alginate is exploited. For example,

upon introduction of Zn^{2+} to a solution containing CaEDTA, calcium will dissociate from its chelate as Zn^{2+} binds more strongly to EDTA than Ca^{2+} (Log K = 16.5 and 10.6, respectively). Additionally, Ca^{2+} binds more strongly to alginate than Zn^{2+}. The dissociated calcium ions will thus be free to form ionic bonds with the alginate chains. Gel strength and gelation time depend on pH and the combination of chelators, gelation ions and exchange ions[62].

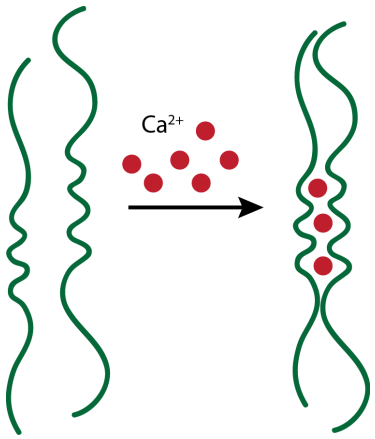

Figure 3.6: Egg-box model of cross-linked alginate chains. Here, repeating G-blocks are represented by a sawtooth shape and calcium ions as red spheres. Two chains of alginate associate as dimers of G-blocks bind to cations on both sides, forming a three-dimensional cross-linked network.

The Navier-Stokes equation (Equation 3.4) presented in Section 3.1 is valid for newtonian, incompressible flow. Alginate solutions, however, are non-newtonian fluids with a non-linear relationship between shear stress and shear rate. More precisely, alginates exhibit a gradual decrease in viscosity with increasing shear rate called *shear thinning*[63]. This inherent property of alginate results in a decrease in viscosity when injected in small-diameter, high-shear microchannel nozzles. Figure 3.7 shows a qualitative description of the relationship between shear stress and shear rate for newtonian and non-newtonian fluids. As illustrated here, there is a newtonian-like viscosity trend for low shear rates[63].

3.4 Microbiological samples

Pseudomonas Putida is a non-pathogenic, biosafe, soil bacterium commonly used for biotechnological applications such as the cloning of foreign genes[64]. When suspended in solution, these bacteria exhibit a motile behavior consisting of unidirectional swimming punctuated by abrupt changes in direction. *Chlamydomonas reinhardtii* are single-celled, green

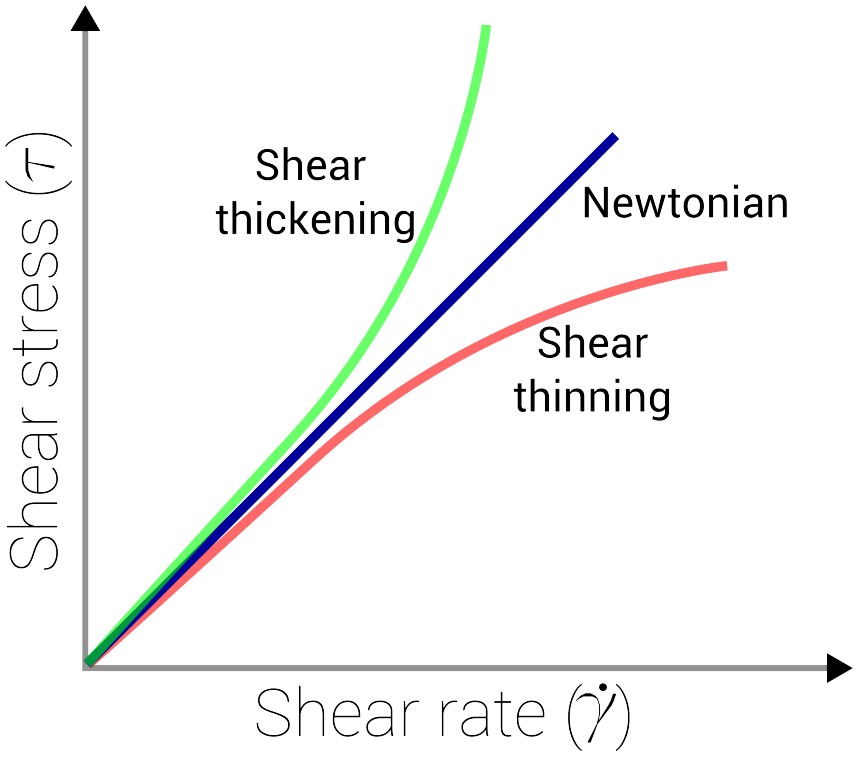

Figure 3.7: Qualitative representation of the behaviour of newtonian and non-newtonian fluids. For newtonian fluids there is a linear relationship between shear stress τ and shear rate $\dot{\gamma}$, where the viscosity μ is given by the slope. Non-newtonian fluids deviate from the linear trend when the shear rate increases; *shear thinning* fluids exhibit a decrease in viscosity as the shear rate increases, while *shear thickening* fluids exhibit an increase in viscosity for increasing shear rate[35].

algae that provide a model system for studies in cell and molecular biology, including cell motility[65]. Both *Pseudomonas Putida* and *Chlamydomonas reinhardtii* move by the aid of multiple flagella, which are lash-like filaments attached to the cell surface or interior[66]. When suspended in water, microorganisms experience low Reynolds numbers and thus move in the laminar regime where viscous forces dominate inertial forces. For Reynolds numbers that approach zero, two properties are crucial for propulsion induced by slender filaments[67]. The first property is drag anisotropy, which allows propulsive forces to be created at a right angle with respect to the local direction of motion of the filament. The second property is a condition that says that the periodic actuation of the filament needs to be non-time reversible in order to generate non-zero forces on average. These properties are the origin of drag-based thrust, which is exploited by *Chlamydomonas reinhardtii* flagella to generate locomotion. *Pseudomonas Putida* flagella are rotating helical structures that lack a mirror symmetry plane. In this case, translational motion is driven through angular forcing[67]. The reader is referred to Lauga and Powers' work "The hydrodynamics of swimming microor-

ganisms", *Reports on Progress in Physics*, 2009[67], for a detailed mathematical elaboration on the underlying fluid dynamics for microorganism motility.

3.5 Microtechniques and fabrication processes

Droplet-based microfluidic devices

Microfluidic devices are commonly fabricated in polydimethylsiloxane (PDMS) using soft lithography, in which liquid PDMS prepolymer is poured over a mould whose surface has been patterned with the complementary structures[68]. The PDMS cures and becomes an elastic solid over time, a process that can be accelerated by increasing the temperature. The moulds are usually masters fabricated by photolithography in a clean room facility, a technique adapted from the semiconductor industry. Conventional photolithography uses UV-radiation to pattern structures larger than 1 µm. A substrate, usually silicon wafers, are coated with a thin layer of UV sensitive photoresist before they are exposed to UV light while covered by masks with the desired pattern. Exposing a negative resist makes it insoluble in a photoresist developer, whereas a positive resist becomes soluble after exposure. When rinsed in photoresist developer after exposure, only the desired structures remain on the substrate which now can serve as a mould for soft lithography. Soft lithography is summarized in Figure 3.8.

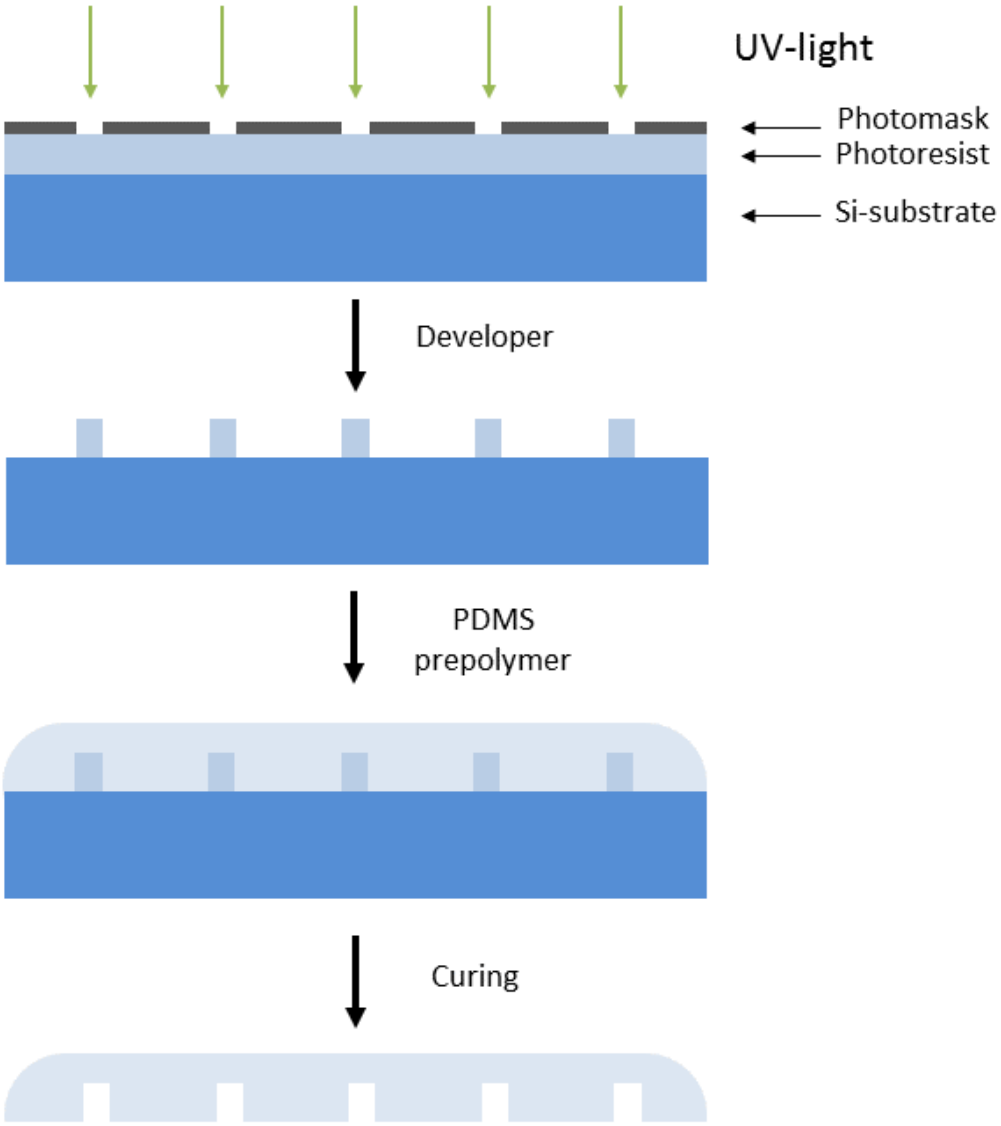

Figure 3.8: Soft lithography: A silicon wafer covered in a negative photoresist is exposed to UV-light while covered by a photomask of the desired pattern. After developing, only the exposed areas remain intact. Liquid prepolymer PDMS is poured over the mould and cured.

The microchannel surface

Synthesis of double emulsions requires a highly controlled wetting pattern. Oil should wet the channel at the water-in-oil junction, which requires a hydrophobic and oil favorable surface. At the second junction however, the outer aqueous phase should wet the channel which requires hydrophilic surface properties. This requires a spatially controlled surface treatment of the double emulsion device. The surface of PDMS is hydrophobic as it contains repeating units of –O-Si(CH_3)$_2$ -groups (Figure 3.9), however, the surface of PDMS can be made hydrophilic by exposing it to oxygen plasma[69]. Oxygen plasma contains many active species that are very effective in breaking most organic bonds, which cleans the surface of organic contaminants and changes the surface bonding chemistry. Exposure to plasma introduces polar silanol(Si–OH) groups on the PDMS surface by destroying the non-polar methyl groups (Si–CH3) (Figure 3.10).

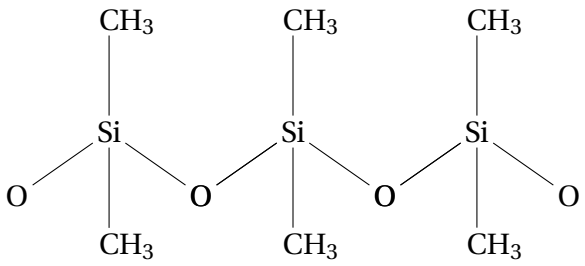

Figure 3.9: Structural formula of untreated PDMS surface[70].

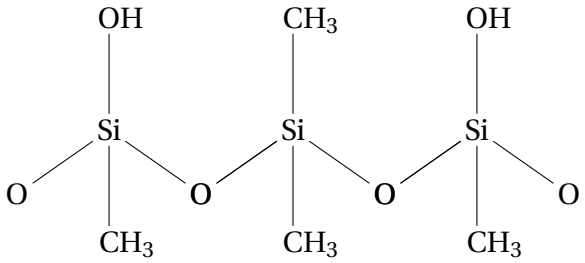

Figure 3.10: Structural formula of PDMS surface after exposure to oxygen plasma[70].

However, the effect is only temporary[71]. The PDMS surface slowly reverts back to being hydrophobic as the Si-OH groups undergo condensation upon exposure of the treated surface to air[70]. It is possible to adjust the surface of PDMS to be hydrophilic over longer time periods, by using different functional groups or to introduce other reactive groups[69]. Deposition of polycations or polyanions have been shown to enhance the lifetime of the hydrophilic PDMS surface[72], in addition to hinder nonspecific molecule adsorption[73]. Furthermore,

exposure to oxygen plasma also allows irreversible bonding of PDMS to PDMS, as the polar silanol groups form covalent O-Si-O-bonds when brought in contact[69]. It is also possible to render the PDMS surface fluorophilic by addition of highly reactive fluorinated silane dissolved in a fluorinated oil. Perfluorodecyltrichlorosilane (Figure 3.11) is hydrolyzed in the presence of OH-groups, converting the Si-Cl bonds to Si-OH (silanol) groups. Subsequently, the silanol groups react with other silanol groups on the surface, creating strong, covalent siloxane bonds. Fluorinated surfaces are both hydrophobic and fluorophilic, making them prone to wetting by oils containing fluoride groups[74].

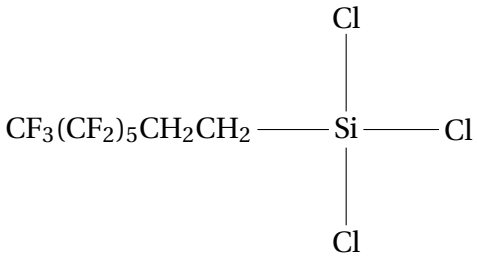

Figure 3.11: Structural formula of perfluorodecyltrichlorosilane (fluorinated silane)[75].

Chapter 4

Methodology

All chemicals were provided by Sigma-Aldrich unless stated otherwise.

4.1 Mask design

The microfluidic device for double emulsion synthesis relies on multiple lithography steps to render 3D features (Section 4.2). Thus, the final device is based on multiple mask designs as shown in Figure 4.1. Features that are present in all three masks will be taller than those present in only two or one, resulting in channels of different heights. The top half and bottom half represent two corresponding slabs of PDMS that are bonded to become the final PDMS device. All designs include protruding triangles and corresponding triangle holes to facilitate alignment for bonding of PDMS-PDMS. The design in Figure 4.1 is the original double emulsion design developed by the Soft Materials Laboratory (SMaL) group at École polytechnique fédérale de Lausanne (EPFL). Figure 4.2a shows a close-up of the same design. In addition to the original design from EPFL, a 3D double emulsion synthesis device with four inlets was designed by Armend G. Håti to allow on-chip mixing of two inner phases. A close-up of this design is shown in Figure 4.2b. Figure 4.3 shows an immobilization array device designed in cooperation with Armend G. Håti to facilitate the study of microbiological activity within an isolated double emulsion assay. The array relies on one lithography step only, and consists of a 80 µm tall channel with an array of 80 µm deep wells covering the channel bottom. The well surface area covers 90 µm × 90 µm. Moreover, the array mask design includes a positioning system consisting of letters and numbers for relocation of a specific area of wells.

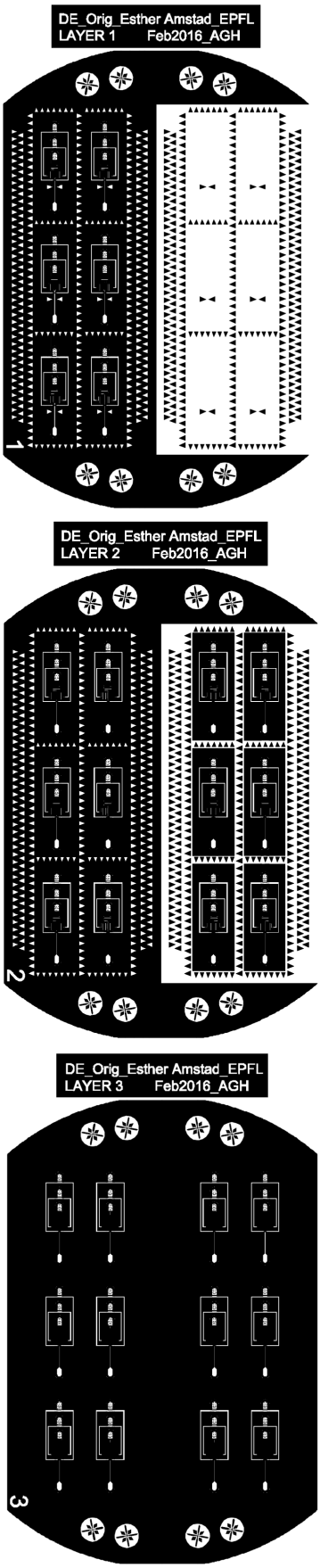

Figure 4.1: Mask designs: Original double emulsion design developed by the SMaL group at École polytechnique fédérale de Lausanne (EPFL). Mask 1 contains all features on the bottom half, and only alignment triangles on the top half. Mask 2 has features on both halves, but lacks the part of the dispersed phase channel that connects the dispersed and continuous phase channels (nozzle). Mask 3 is similar to mask 2, but lacks the upper junction.

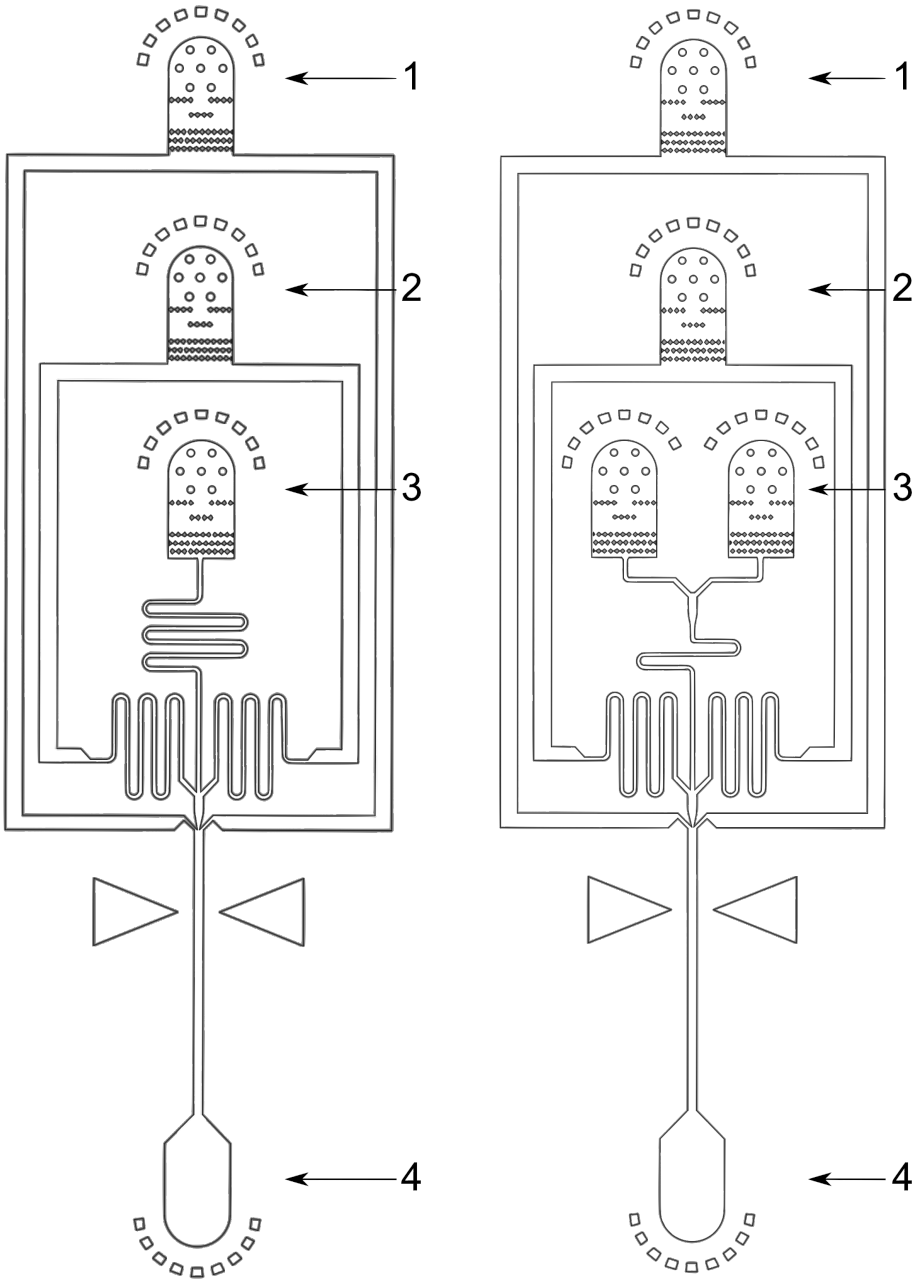

(a) (b)

Figure 4.2: Figure 4.2a: Close-up of the original double emulsion design from EPFL. Figure 4.2b: Close-up of the four inlets device. 1: Outer aqueous phase inlet. 2: Oil phase inlet. 3 (a and b): Inner aqueous phase(s) inlet(s). 4: Outlet. The square dots at the inlets create a mechanical filter designed to inhibit dust particles entering the channels.

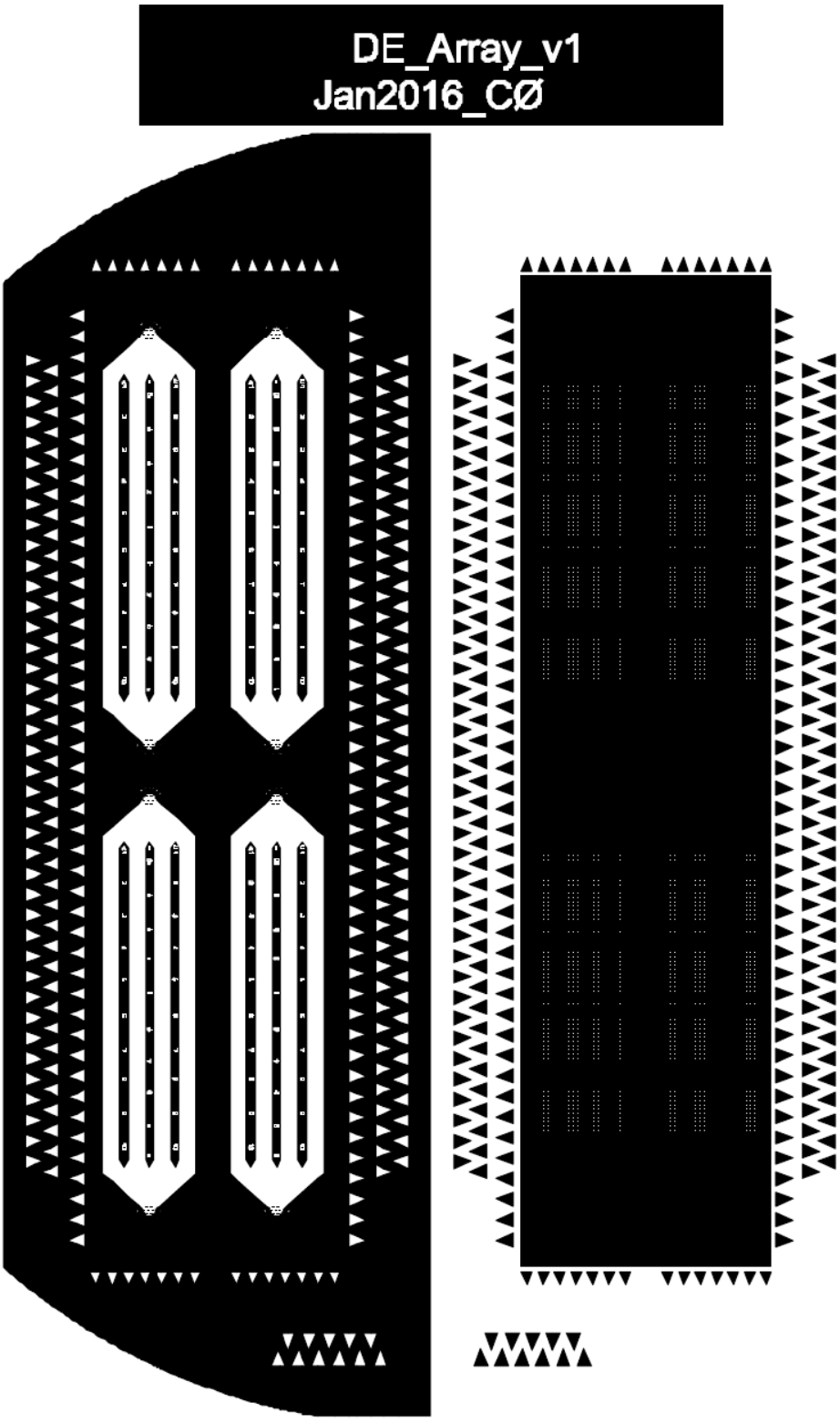

Figure 4.3: Mask design for the immobilization array device. The array consists of a 80 µm tall channel with an array of 80 µm deep wells covering the channel bottom. The well surface area covers 90 µm × 90 µm. The design also includes a positioning system consisting of letters and numbers for relocation of a specific area of wells.

4.2 Fabrication of the double emulsion device

Masters

SU-8 (Micro resist technology) masters were used to mold PDMS devices using soft lithography. Four inch silicon wafers (University Wafers) were cleaned with acetone and isopropanol, and blow-dried with nitrogen before they were exposed to oxygen plasma (Femto PlasmaCleaner, Diener Electronics) for five minutes. After cleaning, the wafers were dehydration baked at 250°C for five minutes before they were spin coated (Spin Coater, Laurell Technologies) with the photoresist SU-8 3050. 20 µm layers were spun for the double emulsion synthesis devices, while a 80 µm layer was spun for the array device. Spin parameters for the different layer thicknesses are shown in Table 4.1. After spin coating, excess SU-8 on the wafer edge was removed by acetone before the resist was soft baked at 65°C for one minute and then at 95°C for fifteen minutes. The wafers were then exposed in a UV maskaligner (MA6, Karl Süss) while covered by a photomask containing the desired design. The exposure energies for the different layer thicknesses are shown in Table 4.2. The resist was post exposure baked at 65°C for one minute and then at 95°C for five minutes. For the 3D double emulsion synthesis devices, the process of spin coating and exposure was repeated twice with different masks to create a three layer mold. Finally, the resist was developed in mr-DEV 600 (Micro resist technology) for six minutes before the wafers were rinsed in fresh developer and isopropanol and blow-dried with nitrogen.

Table 4.1: Spin parameters

Thickness	20 µm:	80 µm:
Ramp step speed [rpm]	500	500
Ramp step duration [s]	10	10
Spin step speed [rpm]	8000	1500
Spin step duration [s]	40	30

Table 4.2: Exposure energies

20 µm	150 mJ cm^{-2}
80 µm	500 mJ cm^{-2}

PDMS

The microfluidic devices were fabricated using soft lithography and the SU-8 masters as molds. The molds were coated with a layer of Trichloro(1H,1H,2H,2H-perfluorooctyl)silane (fluorinated silane) by vapor deposition in a desiccator. Silicon elastomer (Sylgard(R) 184 Silicone Elastomer Base, Dow Corning) and curing agent (Sylgard(R) 184 Silicone Elastomer Curing Agent, Dow Corning) were mixed in a 10:1 ratio for the double emulsion synthesis devices and 5:1 ratio for the array, and thoroughly mixed before degassed in a desiccator. For a four inch wafer in a five inch Petri dish 80 g PDMS was needed for a sufficiently thick device. As the array should be as thin as possible for imaging purposes, about 30 g PDMS was added to a five inch Petri dish. The degassed liquid prepolymer PDMS was poured over the silanized molds, and after removing air bubbles the devices were baked at 65°C for at least two hours to cure. After curing the PDMS devices, they were cut from their molds, punched for inlet and outlet tubes, rinsed for 20 seconds in an ultrasonic bath and finally PDMS-PDMS bonded after 30 seconds exposure to oxygen plasma. The devices were left for bonding at 65°C for 30 minutes. The fabrication process is summarized in Figure 4.4.

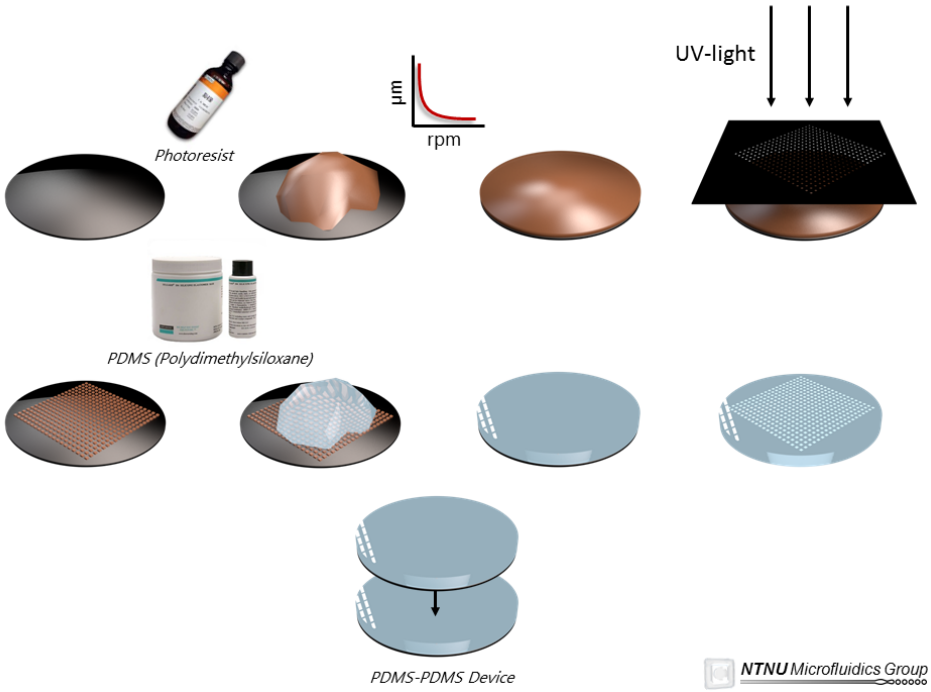

Figure 4.4: Fabrication of devices: Silicon wafer moulds are made by photolithography and used as stamps for imprinting microstructures on PDMS. Courtesy of the NTNU Microfluidics group.

4.3 Surface treatment of the double emulsion synthesis devices

The microchannel surfaces were chemically altered immediately after PDMS-PDMS bonding. The hydrophilic treatment of the outer aqueous phase channel and fluorophilic treatment of the oil phase channel were performed simultaneously and monitored in an inverted optical microscope (Olympus IX70). A pipette tip filled with a polycation solution, poly(diallyldimethylammonium chloride) solution (M_w = 200-350 kDa), dissolved in 2 molar sodium chloride was placed in the outer aqueous phase channel inlet, while a syringe filled with HFE7500 (3M^{TM} Novec^{TM} Engineered Fluid) with 1% (v/v) fluorinated silane was connected to the oil phase inlet. By pulling with an air-filled syringe from the outlet, the channels were filled with their respective solutions, creating HFE7500/silane emulsions in the polycation solution. The pipette tip was continuously refilled with the polycation solution to avoid oil wetting of the outer aqueous phase channel wall. After two minutes the HFE7500/silane solution was replaced with pure HFE7500. The device was then left with HFE7500 in the oil phase channel and polycation solution in the outer aqueous phase channel for another 28 minutes.

4.4 Droplet fabrication

Sample injection was performed by multiple PHD Ultra syringe pumps (Harvard Apparatus). The droplet fabrication was observed in an inverted optical microscope (Olympus IX70) and captured by a Fastcam SA3 high speed camera (Photron). The aqueous samples were dissolved in Milli-Q (Mq) water (Millipore Corporation) for gelation experiments. For encapsulation of bacterial samples or algae, the aqueous samples were dissolved in lysogeny broth (LB) medium (based on a formula described by Miller[76]) or Tris-Acetate-Phosphate (TAP) medium (based on a formula described by the Culture Collection of Cryophilic Algae group at Fraunhofer IZI[77]), respectively. Confocal and fluorescence micrographs were obtained by an inverted fluorescence confocal microscope (TCS SP5, Leica Microsystems) using an argon laser with a wavelength of 488 nm for excitation and a hybrid detector set at 500 nm-600 nm for fluorescence detection. A phase contrast image was obtained with a quantitative phase contrast microscope (Zeiss). Throughout this work, a di-block surfactant with one

fluorine-rich Krytox chain (PFPE) covalently anchored to a PEG chain (900 Da), which were synthesized using a previously described method[39] and generously provided by SMaL at EPFL, was used to facilitate droplet formation and stabilize the double emulsions.

PEG core double emulsions

The chemicals used for the WOW PEG core double emulsions were 20% (w/w) PEG (M_n = 6 kDa) for the inner aqueous phase, HFE7500 with 2% (w/w) surfactant from EPFL for the middle phase and 9.2% (w/w) PVA (M_w = 13-23 kDa) with 100 gL^{-1} sucrose for the outer aqueous phase.

Alginate core double emulsions

Alginate (source *L. hyperborea* stipe) with a guluronic acid residue fraction of F_G=0.68 (PRONTONAL LF 2005, FMC Biopolymer, Haugesund, Norway) and a weight average molecular weight of 275 kDa was dissolved in Mq-water to a final concentration of 3% (w/w). The alginate sample was then further diluted to 0.60% (w/w) or 0.15% (w/w) (pH 6.7) in the medium corresponding to the type of experiment. HFE7500 with 2% (w/w) surfactant was used for the middle phase and 9.2% (w/w) PVA with 100 gL^{-1} sucrose for the outer aqueous phase. In the case of 0.60% alginate cores, 36 mM $CaCl_2$, 36 mM EDTA and 36 mM MOPS were added to the inner aqueous phase, and the amount of sucrose in the outer aqueous phase was increased to 200 gL^{-1}.

Alginate gel initiation

80 mM acetic acid was added to the outer aqueous phase for pH-triggered gelation of 0.60% alginate core double emulsions. Gelation by CLEX was performed in the four inlets device by injecting two 0.60% alginate solutions (pH 6.7)in the inner phase inlets, one containing 36 mM $CaCl_2$, 36 mM EDTA and 36 mM MOPS and the other 36 mM ZnEDDA and 36 mM MOPS. Additionally, gelation by CLEX was attempted by flushing an array of immobilized double emulsions containing 0.60% alginate cores with a solution of 36 mM ZnEDDA, 36 mM MOPS and 9.2% (w/w) PVA with 200 gL^{-1} sucrose.

4.5 Microbiological samples

Bacterial samples

Pseudomonas Putida KT2440 phh100GFP were inoculated and grown overnight (>16 hours) at 30°C in 3 ml LB medium containing 50 mM kanamycin. The optical density (OD) of the bacteria sample was measured at 480 nm by a UV-visible spectrophotometer (UV-visible Spectroscopy System 8453, Agilent Technologies). For an OD_{480} between 0.6 and 0.7, 25 µl of the bacterial sample was added per ml of inner phase fluid. Additionally, 0.5 mM m-Toluic acid was added to the inner phase fluid to initiate green fluorescent protein (GFP) expression.

Algae samples

Chlamydomonas reinhardtii CC-4532 were cultivated in TAP medium at 18 °C and an approximate light intensity of 200 µmol photons $m^{-2} s^{-1}$. The sample was centrifuged (Centrifuge 5415 R, Eppendorf) at 6000 rpm for five minutes, before 200 µl of the centrifuged sample was added per 3 ml of inner phase fluid.

Chapter 5

Results and discussion

5.1 Double emulsion synthesis

Double emulsions were synthesized in 3D microfluidic devices specially designed to facilitate spatially controlled surface treatment and subsequent WOW droplet formation (Chapter 4). In the final 3D design, the inner aqueous phase and oil phase meet at the first junction and enter the continuous phase channel through a nozzle (Figure 5.1). The nozzle cross sectional area is smaller than that of the continuous phase channel, ensuring that the oil is completely surrounded by the outer aqueous phase. The combination of the flow-focusing nozzle and the step at the continuous phase channel entrance facilitates the formation of droplets. Furthermore, the synthesis of WOW double emulsions is promoted by spatially controlled surface treatment. Fluorophilic and hydrophobic treatment of the nozzle channel walls ensures oil wetting in the nozzle, while outer aqueous phase wetting in the continuous phase channel is ensured by a hydrophilic surface treatment. Illustrative videos of double emulsion synthesis and collection can be found in Supplementary Videos.

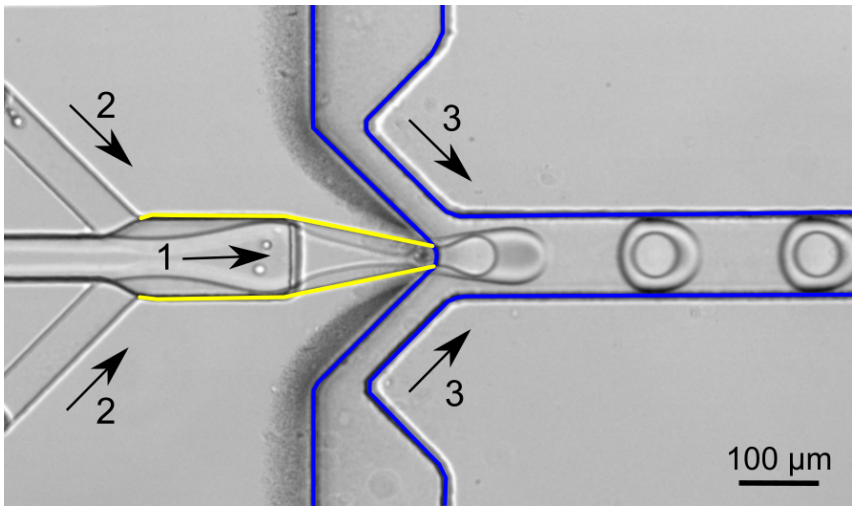

(a)

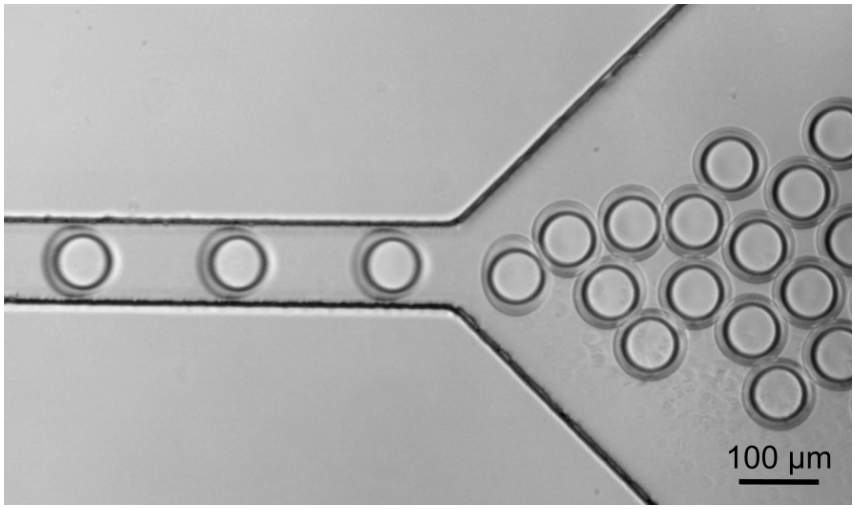

(b)

Figure 5.1: Optical micrographs of the synthesis of double emulsions with an inner aqueous phase (1) and oil phase (2) shells, suspended in an aqueous carrier fluid (3). Formation of double emulsions at the junction between the nozzle (yellow) and continuous phase channel (blue) (Figure 5.1a) is facilitated by 3D geometries as well as spatially controlled surface treatment. Fluorophilic and hydrophobic treatment of the nozzle channel walls ensures oil wetting in the nozzle, while outer aqueous phase wetting is ensured by hydrophilic treatment in the continuous phase channel. The double emulsions are collected at the outlet (Figure 5.1b).

5.2 Double emulsions as biocapsules

Properties of double emulsions

The successful introduction of double emulsions as a platform for studies of biological material relies largely on the characteristics of the double emulsions and their constituents. Firstly, it is imperative that the double emulsions provide a viable, non-toxic environment for living material, that is, they must be biocompatible. All double emulsions synthesized in this work consist of a HFE7500 oil shell, an inert fluorocarbon oil that allows high gas transport which maintains a viable environment for living material that require a continuous supply of oxygen[78]. The solubility of organic molecules on fluorinated oil is normally very low, however, transport through the oil layer is mediated by the presence of surfactants. Nutrients, waste, and other small molecules can therefore be transported in and out of the double emulsions[79]. Secondly, the double emulsions must be stable for a time period exceeding that necessary for the given study. For example, some bacterial proliferation studies require a double emulsion life span of at least eight hours, while algae samples would need several days. As described in Chapter 3, the stability of double emulsions is mainly jeopardized by coalescence, osmotic pressure differences, temperature variations, and shear forces exerted by the carrier fluid. Surfactants in the oil phase as well as the carrier fluid, for example PVA[80], prevent coalescence, in addition to increasing the droplet resistance to shear. Osmotic pressure differences between the double emulsion core and the surrounding media arise as a result of different molar concentration of solutes in the inner and outer aqueous phases. Since the oil layer functions as a semi-permeable membrane, osmotic inequilibrium results in a transport of water molecules in osmotics pressure driven processes. If not accounted for, this unbalance may disrupt the double emulsions, resulting in release of cargo into the surrounding fluid. Here, varying amounts of sucrose was added to the carrier fluid to maintain osmotic pressure equilibrium with respect to the core constituents and cargo. More precisely, for cores consisting purely of PEG or alginate, $100\,\mathrm{g\,L^{-1}}$ was added in an effort to maintain equilibrium. However, when chelates and salts such as CaEDTA and MOPS were present in the double emulsion core, an additional $100\,\mathrm{g\,L^{-1}}$ sucrose were added to a final concentration of $200\,\mathrm{g\,L^{-1}}$. Moreover, the thermostability of the double emulsions was tested as natural metabolic activity and optimal growth of microbes may require incubation at temperatures higher or lower than room temperature. Five parallels of double emulsions

with 20% PEG cores were incubated for one hour at temperatures 5, 10, 37, 50 and 60 °C. All parallels remained stable for the entire incubation time (Figure 5.2). A droplet size analysis provided the outer and inner diameter of the double emulsions presented in Figure 5.2. The results (Table 5.1) display the uniformity of the double emulsions produced in this work. Not all diameters could be determined due to poor image quality.

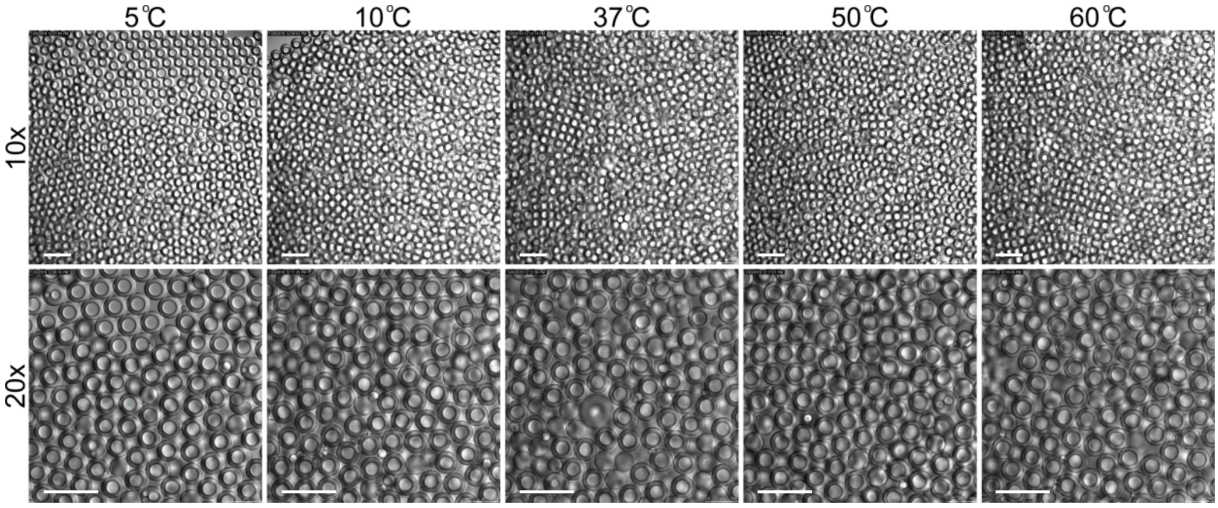

Figure 5.2: Optical micrographs of 20% PEG core double emulsions after one hour incubation at temperatures 5, 10, 37, 50 and 60 °C. Scale bars: 200 µm.

Table 5.1: Outer and inner diameters of the double emulsions from Figure 5.2.

	5 °C	10 °C	37 °C	50 °C	60 °C
Inner diameter [µm]	51.0±1.3	NaN	NaN	50.1±1.4	50.8±1.3
Outer diameter [µm]	78.4±1.2	78.0±1.0	78.2±0.9	70.4±5.0	78.7±1.5

Finally, certain applications of double emulsions require a high resistance to shear-induced destabilization, such as the use of double emulsions as compartments for flow cytometry[46]. A flow cytometry analysis of double emulsions containing 20% (w/w) PEG cores with LB medium is presented in Appendix B. Furthermore, double emulsions were successfully immobilized on microarrays by syringe injection without being destabilized by shear (Figure 5.3). The array presents a simple and quick method for immobilization, as double emulsions suspended in a less denser medium will sediment in the channel and subsequently be immobilized in the wells.

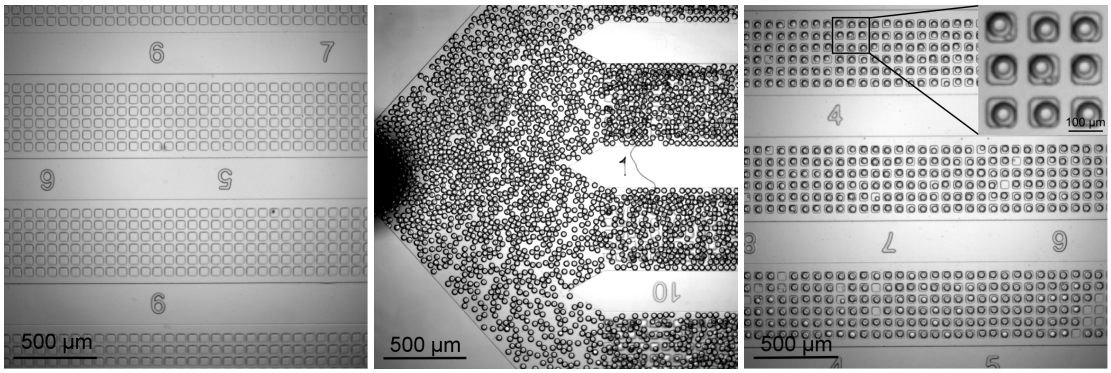

(a) (b) (c)

Figure 5.3: Optical micrographs of the empty array (Figure 5.3a), filling of the array with double emulsions (Figure 5.3b) and the filled array after flushing with water containing 100 gL^{-1} sucrose (Figure 5.3c).

Controlling size and multiple cores

Biocapsules of varying and controllable sizes may be needed depending on the type of cargo. In a stable microfluidic system, the double emulsion size, both the inner and outer diameter, may be fine-tuned by adjusting the viscosity of fluids, channel geometries, as well as the flow rates of the different phases. A device was considered stable when double emulsions were produced in a controlled manner and fine-tuning of the core and shell thickness was possible by varying the flow rates. Table 5.2 shows different outer and inner diameters of 0.60% alginate core double emulsions for varying flow rates, all synthesized in the same device. A more thorough analysis of the relationship between the flow rates and droplet size lies outside the scope of this thesis. In this work, double emulsions between roughly 50 µm and 100 µm in outer diameter and 20 µm and 80 µm in inner diameter were synthesized, which are suitable dimensions for flow cytometry [81] and microarrays (90x90 µm). Moreover, flow rates and viscosities may be adjusted to control the number of alginate cores within each oil droplet. Figure 5.4 displays the synthesis of multiple 0.60% alginate cores at different flow rates. It was found that the main component controlling the number of alginate cores was the carrier fluid (PVA) flow rate. Precise relationships between the flow rates and droplet size, as well as between flow rates and the number of cores, were generally difficult to determine due to unstable devices. Unstable devices produced double emulsions of varying sizes and number of cores at fixed flow rates, as the one depicted in Figure 5.4. Variations from device to device were also observed. The variations in device performance were likely due to alignment of the PDMS chip, surface treatment, defects in the inlet tubes with regards to

differences in hydrodynamic resistance, or a combination thereof.

Table 5.2: Outer and inner diameter of 0.60% alginate core double emulsions for different flow rates.

PVA flow rate [$\mu L h^{-1}$]	HFE7500 flow rate [$\mu L h^{-1}$]	Alginate flow rate [$\mu L h^{-1}$]	Outer diameter [µm]	Inner diameter [µm]
1000	200	100	87.5	51.6
1000	100	100	70.1	47.8
800	100	50	89.2	64.6
600	100	100	88.0	58.0

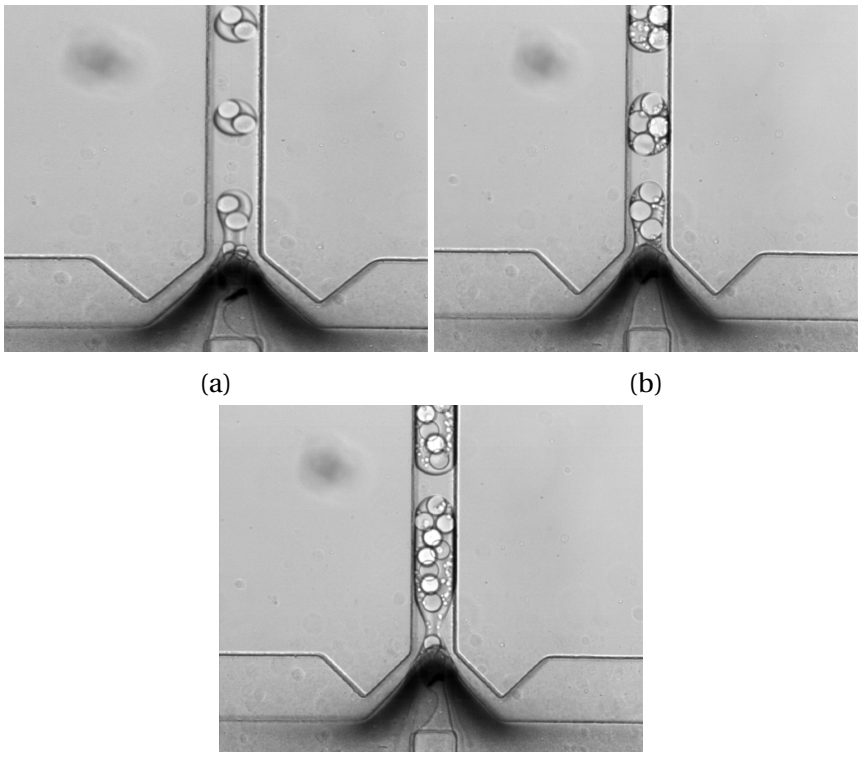

(a) (b)

(c)

Figure 5.4: Optical micrographs of the formation of multiple alginate cores in double emulsions. The number of alginate droplets varied with flow rates, however, no definite relationship could be determined. Figure 5.4a: PVA 500 $\mu L h^{-1}$, oil 300 $\mu L h^{-1}$ and alginate 100 $\mu L h^{-1}$. Figures 5.4b and 5.4c: PVA 100 $\mu L h^{-1}$, oil 50 $\mu L h^{-1}$ and alginate 50 $\mu L h^{-1}$.

The nozzle represents a constriction accompanied by an increased shear exerted on the fluids. The resulting flow profile of PEG is given by the solution of the Stokes equation (Equation 3.5). Alginate however, exhibits a non-newtonian behaviour yielding a more curved flow-profile compared to that of PEG upon an increase of shear. The non-newtonian behaviour

of alginate can be observed in Figure 5.5. Due to the shear thinning properties of alginate, jet dripping was frequently observed in the nozzle tip. This effect made the double emulsion synthesis more difficult to control, and occasionally resulted in the formation of numerous alginate cores within a single oil droplet.

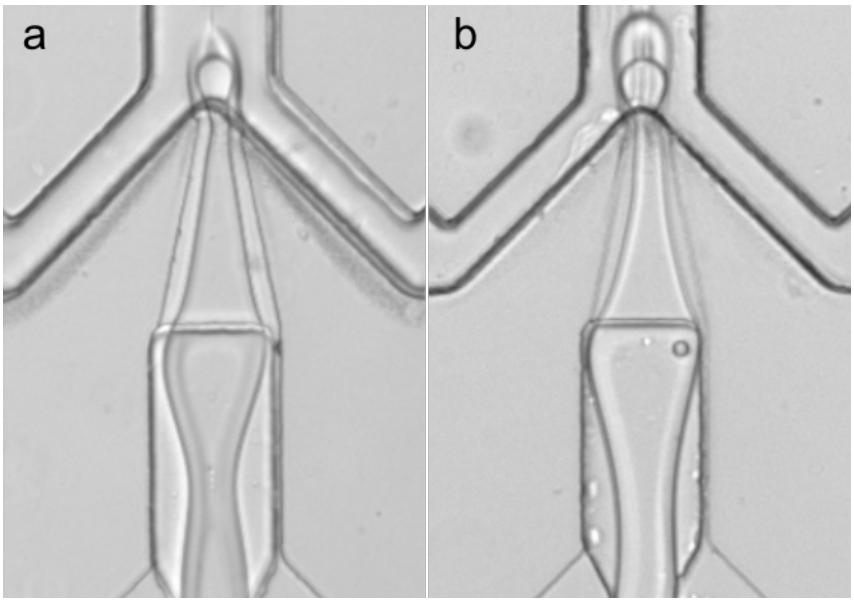

Figure 5.5: Flow profiles of 20% PEG (a) and 0.60% alginate (b). The shear increases as the fluids flow through the nozzle, which in both cases increases the flow velocity. Alginate however, experiences additional non-linear changes in viscosity due to shear thinning effects resulting in a curved flow profile and jet dripping in the nozzle tip (b). The thinning of the jet observed upstream of the nozzle is due to viscous forces exerted on the PEG and alginate flows by the oil phase.

5.3 Gelation of double emulsion core(s)

Under certain conditions, double emulsion alginate cores can undergo cross-linking for the synthesis of spherical, micron-sized hydrogels. Hydrogels of controllable size and shape serve many purposes in biotechnology, microbiology and medicine, such as tissue engineering and cell-based drug delivery[11]. Double emulsions are widely applied as templates for the synthesis of liposomes[82] and polymersomes[51], structures that mimic the membrane of the cell. Hydrogel cores may therefore serve as templates to synthesize mimics of the cell body[83]. Gelation of alginate cores can be done externally or internally, as described in Chapter 3, however, internal gelation is the method evaluated here as it is favorable for microfluidic systems[58][59].

pH-triggered gelation

The internal pH of microdroplets can be controlled externally by exploiting the diffusive exchange of reactants that are soluble in both the oil and aqueous phase. Acetic acid has been shown to display significant solubility in both water[84] and fluorinated oil[85]. The solubility properties of acetic acid are particularly useful for triggering a timed decrease in pH in a microdroplet system, as they permit a flux through both phases. Here, internal gelation of 0.60% (w/w) double emulsion alginate cores was initiated by introducing chelated Ca^{2+} ions in the alginate precursor solution. EDTA was used to chelate Ca^{2+} ions close to neutral pH (6.7) as Ca^{2+} has a higher affinity towards this chelate than the alginate chain at these conditions[62]. As a flux of acetic acid (80 mM) from the continuous phase through the oil layer lowers the internal pH, Ca^{2+} ions and EDTA dissociate[86], leaving the Ca^{2+} ions free to gel the alginate chains in the double emulsion core. The double emulsions were collected and imaged shortly after synthesis (Figure 5.6). The red arrows in Figure 5.6 indicate interfaces between alginate gels and surrounding water layers resulting from a shrinking as gelation progressed. It would also be possible to initiate gelation at a later stage by immersing the double emulsions in PVA containing acetic acid post-synthesis. Gelation triggered by altering the pH offers a reliable and rapid method for on-chip gelation of alginate cores, however, the method may be unfavorable for biomacromolecules that are sensitive to pH changes[87][58]. Moreover, spherical alginate microgel clusters were synthesized by pH-triggered gelation of multiple 0.60% alginate cores (Figure 5.7). Figure 5.7a shows dou-

ble emulsions containing three and four cores at the outlet of the collection channel. After synthesis, the double emulsions were collected and destabilized in bulk by disturbing the osmotic pressure equilibrium through the addition of pure water, leaving free spherical alginate microgel clusters in solution (Figure 5.7b). Such clusters may potentially find use in hierarchical structuring of microgels for tissue engineering purposes[88].

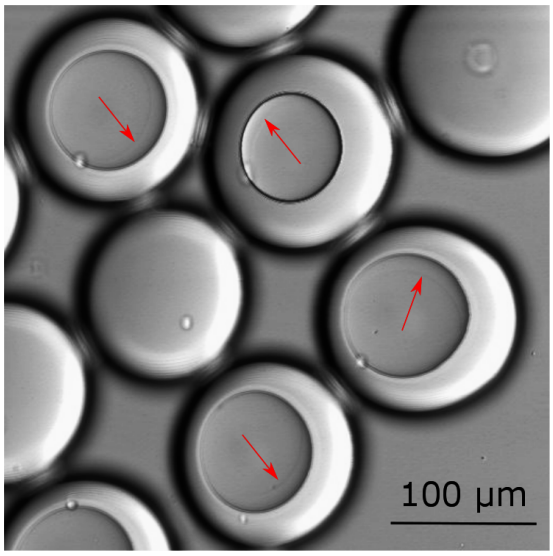

Figure 5.6: Confocal micrograph of cross-linked double emulsion cores. Gelation of 0.60% alginate cores containing CaEDTA was triggered by adding acetic acid to the continuous phase. The red arrows indicate the interfaces between the alginate gels and surrounding water layers.

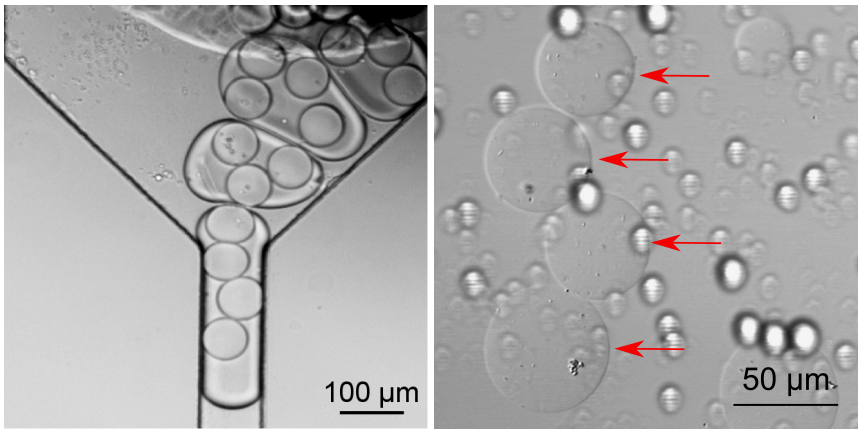

(a) (b)

Figure 5.7: Figure 5.7a: Optical micrograph from the synthesis of double emulsions containing three and four alginate cores. The flow rates used were 150 µLh^{-1} for PVA, 100 µLh^{-1} for HFE7500 and 125 µLh^{-1} for alginate. Figure 5.7b: Confocal micrograph of spherical alginate microgel clusters synthesized by pH-triggered gelation of multiple 0.60% alginate cores.

CLEX

Compared to pH-triggered gelation, CLEX is a more biocompatible internal gelation method as the pH remains unchanged during the gelation process. Moreover, as CLEX offers more controlled gelation kinetics, the risk of clogging the device is substantially decreased[59]. Here, two methods of introducing the exchange ion were tested; either via the carrier fluid and transport through the oil layer or via separate inner phase inlets. The former method was tested post-synthesis on immobilized double emulsions with 0.60% alginate cores containing 36 mM CaEDTA and 36 mM MOPS by flushing with ZnEDDA (36 mM) and MOPS (36 mM) and 100 gL^{-1} sucrose (Figure 5.8). However, the flux of chelated zinc through the oil layer was insufficient to initiate gelation before the double emulsions collapsed due to differences in osmotic pressure between the core and surrounding medium. As a result, long-term monitoring of the ZnEDDA flux and subsequent gelation of the core was hindered. As an attempt to overcome this obstacle, two surrounding medium controls were performed; one with 10% PVA and 100 gL^{-1} sucrose in water, and one with only 100 gL^{-1} sucrose in water to test the effect of 10% PVA on droplet stability. The double emulsions were unstable in both controls, indicating that the addition of 10% PVA had little or no effect. The decrease in osmotic stability compared to previous experiments may be due to the addition of 36 mM CaEDTA and 36 mM MOPS in the alginate cores, and could possibly be accounted for by increasing the amount of sucrose in the surrounding medium. Disregarding the instability issue, when the transport of exchange ions across the oil layer is too slow, there is still the matter of potential leakage of chelated gelling ions from the double emulsion core. This method of gelation was therefore not tested any further.

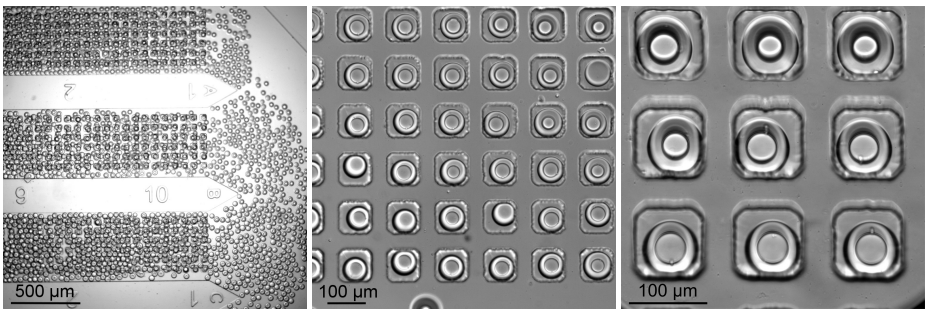

(a) Filling the array (b) (c)

Figure 5.8: Optical micrographs of filling of the array with double emulsions (Figure 5.8a), the filled array after flushing with 36 mM ZnEDDA and 36 mM MOPS and 100 gL^{-1} sucrose (Figure 5.8b) and a close-up of the filled array (Figure 5.8c).

A four inlets device with two inner aqueous phase inlets was designed for a more efficient application of the CLEX method for gelation of 0.60% alginate cores. Double emulsions were synthesized using the four inlets device with two 0.60% alginate solutions with 36 mM MOPS (pH 6.7) as the inner phases, one containing the chelated gelling ion (CaEDTA) and the other the chelated exchange ion (ZnEDDA) at the same concentrations as above. Compared to the original double emulsion synthesis device, the four inlets device was more difficult to control due to the two alginate flows. Firstly, the additional inlet decreased the hydrodynamic resistance when unconnected. Thus, the device was more prone to oil backflow in the inner phase channel when initiating the synthesis of oil droplets in water at the start of a microfluidic experiment. Secondly, even small differences in the two alginate inlet tube lengths resulted in backflow of one alginate phase into the other. Figures 5.9a and 5.9b show the combined effect of these two; alternating oil and alginate plugs are formed in the inner phase junction destabilizing both the co-flow and droplet formation further downstream in the nozzle junction. However, by carefully matching the alginate inlet tube lengths and given enough time to stabilize (several minutes), the device successfully synthesized double emulsions (Figure 5.10). The double emulsions were destabilized post-synthesis by addition of pure water, thus separating gelled alginate cores from the oil layers (Figure 5.10c). Here, not all double emulsions are destabilized, as the destabilization process occurs randomly and over time. The four inlets device represents a more cumbersome gelation method, but offers a controlled and well-timed gelation process suitable for microfluidic systems. Furthermore, having two inner phase inlets introduces the possibility of on-chip mixing of cargo constituents for encapsulation experiments. For example, two different types of bacteria can be injected in the system separately and subsequently mixed as the double emulsions are formed. This facilitates studies of bacterial interaction processes as the time of contact is delayed.

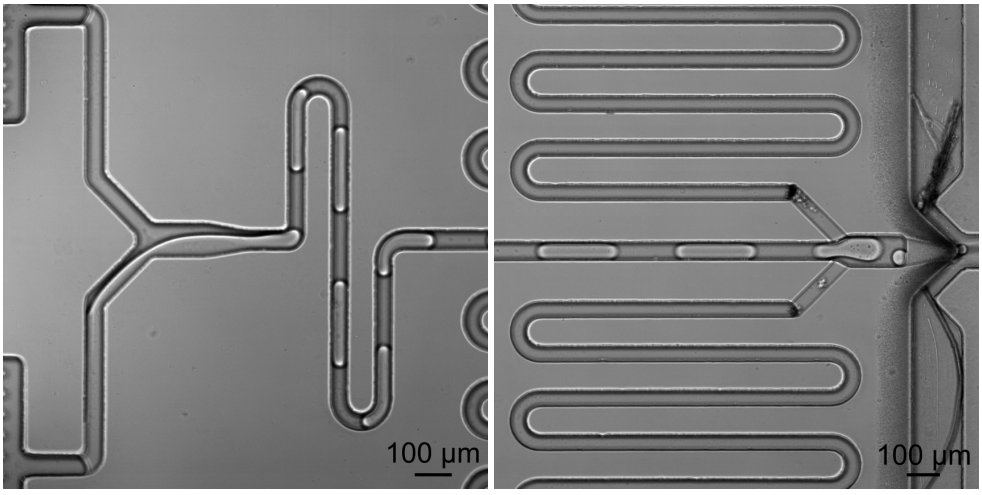

(a) (b)

Figure 5.9: Optical micrographs of unstable flows in the four inlets device. Compared to the original double emulsion synthesis device, this device was more prone to backflow. The result was a formation of plugs which destabilized the system and inhibited a continuous synthesis of double emulsions. A dust particle has entered the continuous phase channel in Figure 5.9b. Such particles may disrupt the flow and destabilize the system, however, dust particles were often trapped in the inlet filters.

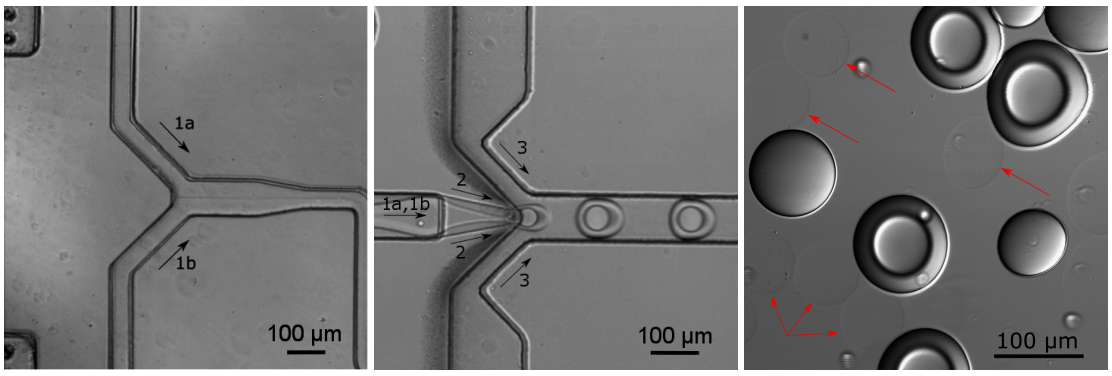

(a) (b) (c)

Figure 5.10: Figure 5.10a: 0.60% alginate containing CaEDTA (1a) and ZnEDDA (1b) co-flows through the junction and mixes in the inner phase channel. Figure 5.10b: Formation of alginate droplets containing CaEDTA and ZnEDDA (1a,1b) with HFE7500 (2) shells suspended in a PVA solution containing 100 $g L^{-1}$ sucrose (3). Figure 5.10c: Spherical microgels (red arrows) formed by CLEX in the four inlets device. Not all double emulsions are destabilized, as the destabilization process occurs randomly and over time.

5.4 Encapsulation of microorganisms in double emulsions

To test the suitability of double emulsions as microbial capsules, *Pseudomonas Putida* and *Chlamydomonas reinhardtii* algae were encapsulated and monitored over time. Different constituents and concentrations of the inner and aqueous phases, as well as their additional solutes, were varied to optimize both the microenvironment and double emulsion stability.

Cell encapsulation rates

As the cells are suspended in the inner phase fluid, their spacial distribution and timing of arrival at the droplet formation site is essentially random for this encapsulation method. The cell encapsulation rate is governed by a Poisson distribution, where the average number of encapsulated cells per droplet increases with cellular concentration[5]. More importantly, the Poisson distribution states that as the cellular concentration approaches a lower limit, few of the double emulsions will contain cells, though a large portion of these will contain single cells. Thus, to optimize single cell encapsulation, the cellular concentration should be kept at the limit for efficient throughput and maximum single cell encapsulation, and a downstream sorting system such as acoustofluidic[89] or dielectrophoretic[90] FACS should be developed to produce an exclusively single-cell droplet population. Here, the optical density of the bacterial samples was measured before mixing with the inner phase fluid to maintain the same cellular concentration for all experiments. As no sorting system was applied, the cellular concentration was kept relatively high to ensure high throughput of cell-containing double emulsions. For bacterial encapsulation, most double emulsions thus contained few, but more than one cell after synthesis.

Suitable double emulsion core material for *Pseudomonas Putida*

Pseudomonas Putida were encapsulated in double emulsions using 20% PEG for the inner aqueous phase and imaged first 30 minutes after encapsulation by a fluorescence confocal microscope (Figure 5.11, top) and subsequently by a quantitiave phase microscope (Figure 5.11, bottom). Single oil emulsions are present in the latter micrograph, probably due to poor osmotic stability over time. For 20% PEG cores no swimming bacteria were observed even shortly after encapsulation, indicating that the conditions were unfavorable for this type of bacteria. What is more, all bacteria in Figure 5.11 are located in the same focal plane, which is

a strong indication of cell death and sedimentation within the double emulsion core. It was therefore concluded that PEG provided a toxic environment to *Pseudomonas Putida*, and the use of PEG in the inner phase was discontinued.

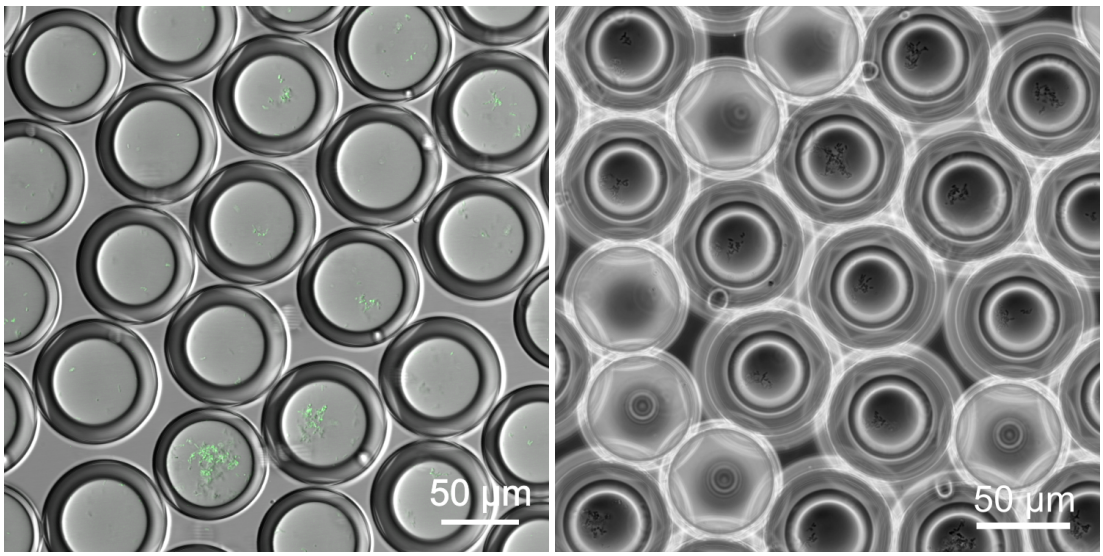

Figure 5.11: Clusters of *Pseudomonas Putida* encapsulated in 20% PEG core double emulsions imaged by a confocal fluorescence microscope (top) and a quantitative phase contrast microscope (bottom). The bacterial activity was low even shortly after encapsulation, and the use of PEG for the inner phase was discontinued.

PEG was replaced in the inner phase by 0.15% alginate which is known to be non-toxic and biocompatible (Section 3.3). Alginate exhibits viscosities suitable for droplet formation at a wide range of concentrations (concentrations from 0.15% to 1.00% were tested). However, as the alginate concentration increased, difficulties in maintaining a steady and controlled co-flow through the microchannel nozzle due to shear thinning effects became evident. Therefore, the concentration of alginate was kept at a minimum for pure encapsulation experiments to enable smooth and continuous double emulsion synthesis. Figure 5.12 shows overlapped fluorescence and bright field images of bacteria growth over 24 hours after encapsulation. As the double emulsions were imaged in bulk, the emulsions depicted at 0 hours and 24 hours are not the same. However, Figure 5.12 represents a general growth of bacteria within the emulsions, indicating that alginate is a more suitable medium for encapsulation of *Pseudomonas Putida* than PEG. Additionally, swimming bacteria were observed in the double emulsions shortly after synthesis (Supplementary video 1). Just as for PEG, the alginate core double emulsions exhibited an osmotic pressure imbalance over time, as depicted by the leaked bacteria after 24 hours in Figure 5.12. It is possible that the osmotic sta-

bility could have been enhanced both for PEG and alginate cores by increasing the amount of sucrose in the carrier fluid. To resolve the relocation issue related to bulk imaging, the double emulsions were immobilized on a PDMS microarray. Figure 5.13 shows double emulsions containing *Pseudomonas Putida* in 0.15% alginate cores immobilized on an array. The array was flushed with 9.2% PVA dissolved in LB with 100 gL^{-1} sucrose and imaged every hour to monitor bacteria growth. Growing colonies and swimming bacteria (Supplementary video 2) were observed in all nine double emulsions after two hours, however, after four hours some of the double emulsions burst and released the bacterial cargo. The colonies that remained encapsulated seemed to grow steadily over the course of the four hours they were monitored. Figure 5.14 shows a close-up of the framed double emulsion from Figure 5.13. After five hours only two double emulsions remained, and the experiment was therefore terminated. These results show that 0.15% alginate core double emulsions are suitable for encapsulation of *Pseudomonas Putida*, albeit there is an osmotic pressure instability issue to resolve.

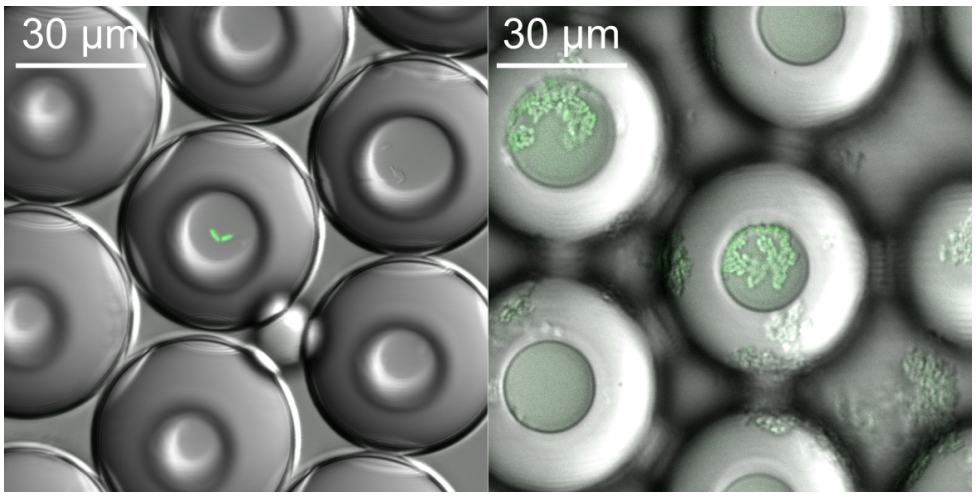

Figure 5.12: Overlapped fluorescence and bright field micrographs of *Pseudomonas Putida* growth in 0.15% alginate core double emulsions 0 and 24 hours after encapsulation. The double emulsions were imaged in bulk, meaning that the ones imaged at 0 hours and 24 hours are not the same. After 24 hours some bacteria had leaked, indicating an osmotic pressure inequilibrium in the system.

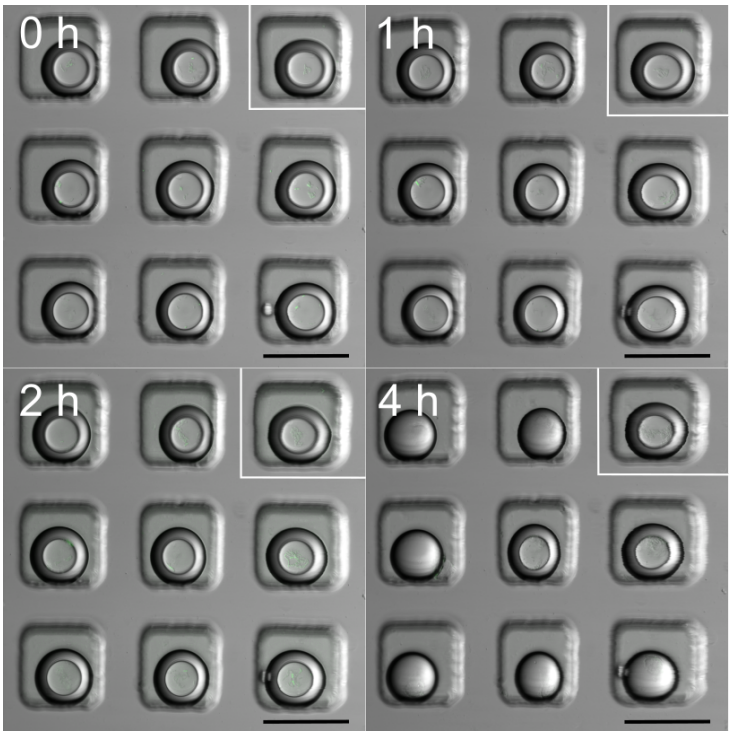

Figure 5.13: Overlapped fluorescence and bright field micrographs of immobilized double emulsions containing *Pseudomonas Putida* in 0.15% alginate cores. Bacterial growth was observed over four hours, however, osmotic pressure instability hindered a complete examination of growth in all nine double emulsions. Scale bars (black): 100 µm.

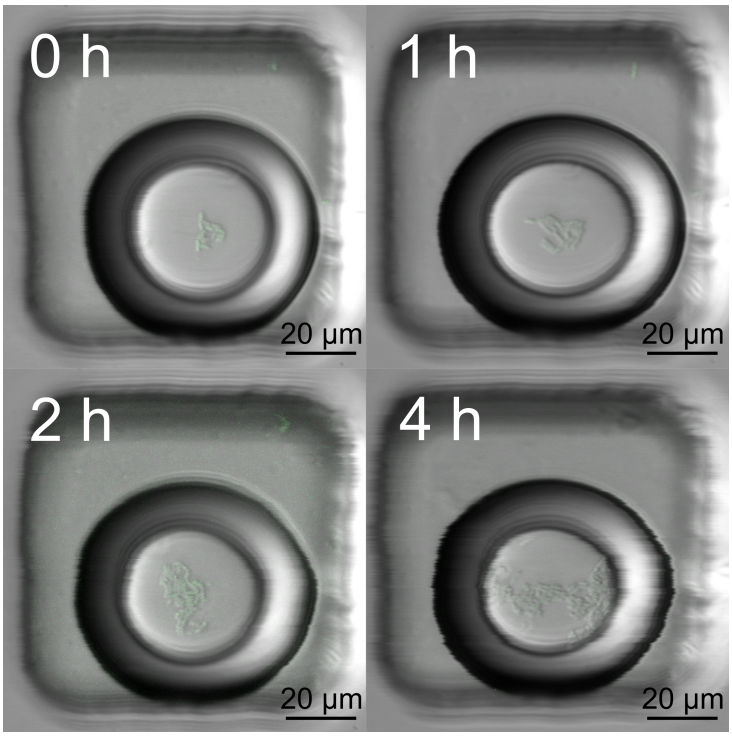

Figure 5.14: Close-up of the framed 0.15% alginate core double emulsion from Figure 5.13. The colonies grew steadily over the course of four hours. Image recording was in some cases (e.g. bottom right) disturbed by fluctuations in the surrounding media.

Encapsulation of *Pseudomonas Putida* in 0.60% alginate cores

As previously mentioned, spherical, micron-sized hydrogels may serve many useful purposes within fields such as medicine, biotechnology and microbiology. CLEX and pH-triggered gelation as described above yield gelation shortly after synthesis, however, in some cases it might be purposeful to delay the gelation process. For example, by initially allowing the cells to move freely and interact with each other, processes like bacterial conjugation can be studied[91]. Gelation can later be triggered by flushing an array of immobilized double emulsions containing 0.60% alginate cores with an acidic solution if a pH-triggered gelation strategy is used. By fixating the cargo within an alginate hydrogel network, image resolution is enhanced and more detailed information about the effects of the specific cellular process may be obtained. Since gelation is delayed until the cellular process has been terminated, bacterial viability is less of a concern and gelation can be triggered by decreasing the pH. *Pseudomonas Putida* were therefore encapsulated in 0.60% alginate cores, an experimentally observed lower limit for gelation of the alginate used in this work[59], for growth monitoring and subsequent alginate gelation. The double emulsions were observed in bulk immediately after encapsulation to monitor cell activity and movement. However, compared to what was observed in 0.15% alginate cores, the bacteria seemed immobile. The external viscosity was presumably too high to allow for bacterial motility[92]. To further investigate the encapsulated bacteria, double emulsions were immobilized following the same procedure as for 0.15% alginate cores and flushed with 9.2% PVA dissolved in LB with 200 $\mathrm{g\,L^{-1}}$ sucrose (Figure 5.15). The amount of sucrose was increased by 100 $\mathrm{g\,L^{-1}}$ in an attempt to balance the osmotic pressure differences previously observed for PEG and 0.15% alginate core double emulsions. The double emulsions remained intact over four hours, however, no bacterial growth was observed (Figure 5.16). Gelation was not attempted as the experiment was terminated when it was apparent that the bacteria did not proliferate under these conditions.

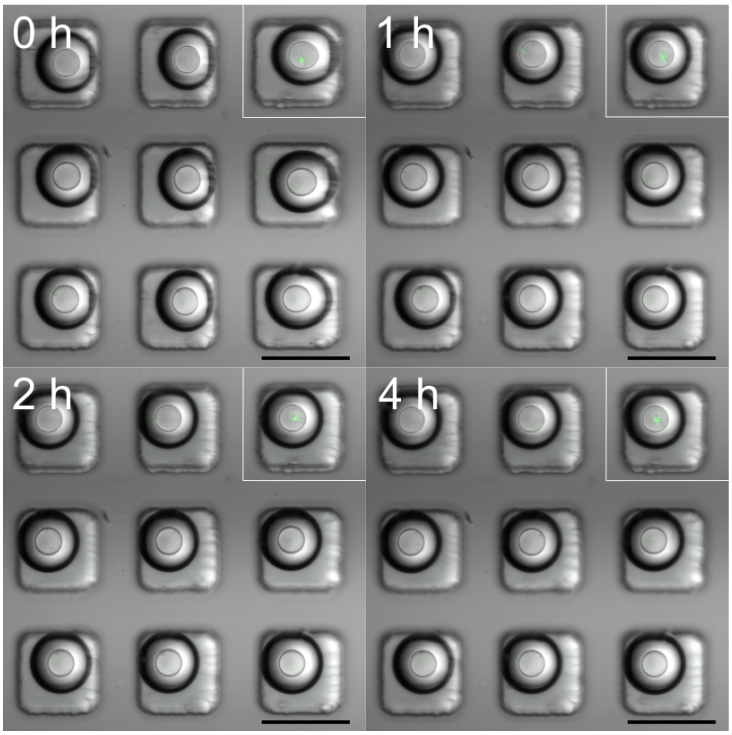

Figure 5.15: Overlapped fluorescence and bright field micrographs of immobilized double emulsions containing *Pseudomonas Putida* in 0.60% alginate cores. The double emulsions remained intact over four hours, however, no bacterial growth was observed. Scale bars (black): 100 µm.

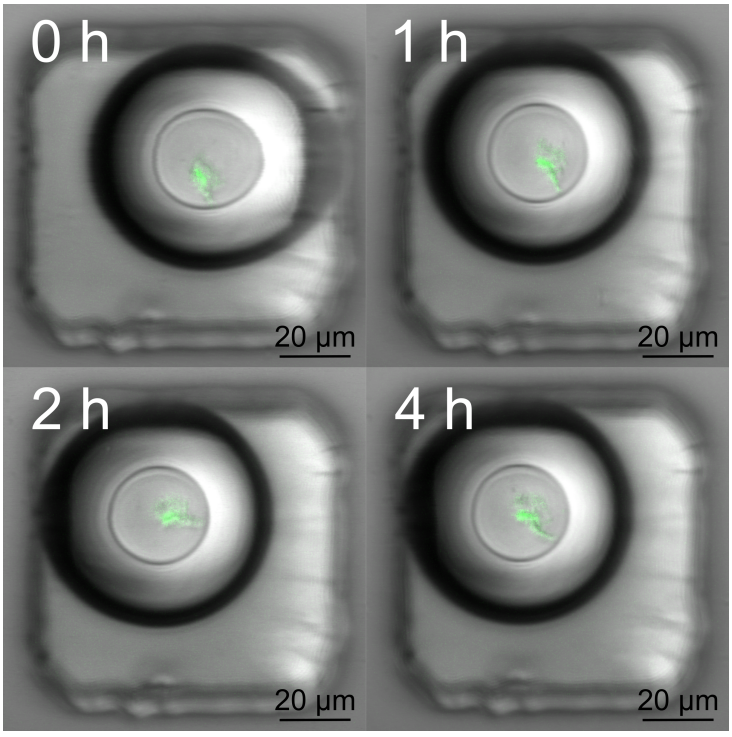

Figure 5.16: Close-up of the framed 0.60% alginate core double emulsion from Figure 5.15. Gelation was not attempted as no bacterial growth was observed under these conditions.

Encapsulation of *Chlamydomonas reinhardtii* in 0.60% alginate cores

Chlamydomonas reinhardtii were encapsulated in double emulsions with 0.60% alginate cores to investigate the algae motility and proliferation rate, as cores that may subsequently be gelled were desired. Some algae motility was detected immediately after encapsulation (Supplementary video 3), although decidedly reduced compared to algae motility in pure TAP medium (Supplementary video 4). Furthermore, no cell division was observed after 24 hours incubation in the double emulsions, as exemplified by the two algae in Figure 5.17. Additionally, the double emulsions were less stable in the surrounding media containing TAP than was the case for *Pseudomonas Putida*. This may be attributed to different amount of osmotically active components for TAP compared to LB[77][76]. Screening tests with varying amounts of sucrose added to the outer phase were therefore conducted, however, no improvement with respect to double emulsion stability was observed. Presumably, the TAP medium destabilizes the fluorosurfactant. Since TAP consists of large amount of salts[77], the amount of free ions in solution are significantly higher than in LB medium[76]. Free ions in solution may order the water structure and thereby lower the cloud point of PEG 3.2, which consequently destabilizes the surfactant and causes rupture of the double emulsions.

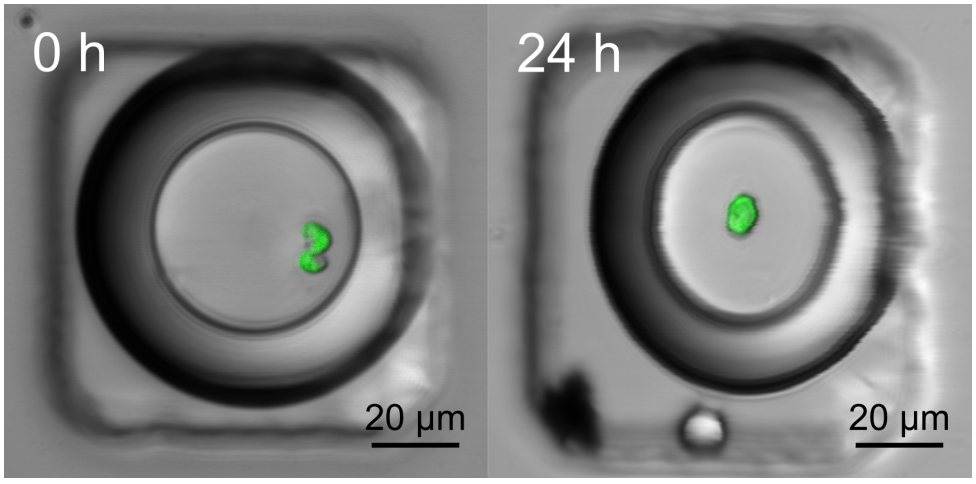

Figure 5.17: Overlapped fluorescence and bright field micrographs of an encapsulated algae after 0 hours and one after 24 hours of encapsulation, which demonstrate that no cell division has occurred in the sample after 24 hours.

5.5 Evaluation of current challenges

Although 0.15% alginate core double emulsions yielded promising results as microcapsules for bacterial compartmentalization, osmotic pressure instability remains a major issue. However, by conducting a series of screening tests, the necessary amount of added sucrose could be determined for the specific experiment such that osmotic pressure differences can be accounted for and double emulsion stability is enhanced. Ideally, the osmolarities of the inner and outer aqueous phases should be determined by an osmometer for a more efficient and precise determination of the amount of molecules present in each phase, which would eliminate the need for screening tests. This approach has for example been demonstrated by Martino and co-workers[83]. Furthermore, the effect of TAP on surfactant dynamics should be examined for encapsulation of algae.

The rate of single cell encapsulation was not determined in this work. As no filtering system was applied, the cellular concentrations were kept relatively high to ensure high throughput of cell-containing double emulsions. Most double emulsions depicted in this chapter therefore contain more than one cell at time zero, although in low numbers. Additionally, due to practical timing issues, it is reasonable to assume that some bacterial proliferation occurred before the double emulsions were immobilized and ready for imaging. For improved single-cell encapsulation rates, a downstream sorting system should be developed. Standing surface acoustic wave-based (SSAW) microfluidics was briefly tested for this purpose. Preliminary results indicate the possibility of manipulating double emulsions with acoustic waves as can be seen in Supplementary Video 5, however rigorous testing of this system still remains.

Even though both bacterial and algae samples have successfully been grown in hydrogels, neither seemed to display proliferation tendencies in 0.60% alginate core double emulsions. This could be attributed to the high viscosity of the sample which inhibits movement and prevents the microorganisms from interacting and finding anchoring points. As explained in Section 3.4, microorganisms in suspension in a viscous medium experience a local laminar regime, where movement is largely dependent on viscous forces. Another possibility is that the flow of nutrients through the double emulsions shell is insufficient to provide appropriate conditions for cell survival and proliferation. Hydrogels on the other side, display

more permeable characteristics due to the porous polysaccharide network which allows a higher flux of nutrients. Still, double emulsions could be a useful platform for encapsulation and delayed fixation in gelled alginate cores for other types of microorganisms not tested here.

Chapter 6

Conclusions and further work

Compartmentalization of cells in small, confined volumes yields a more comprehensive understanding of a variety of cellular processes and properties of the individual cell than traditional bulk studies. Methods for single-cell studies are therefore constantly being developed and optimized to provide viable microenvironments for cell encapsulation, as natural metabolic activity and growth is of paramount importance if cellular processes like bacterial conjugation are to be studied.

Spherical, micron-sized hydrogels were synthesized through gelation of double emulsion alginate cores. Gelation was initiated by the addition of acetic acid to the outer aqueous phase and chelated Ca^{2+} ions in the inner aqueous phase, the latter phase consisting of 0.60% high G-content alginate. Confocal micrographs revealed the formation of an interface between alginate gels and surrounding water layers in intact double emulsions, as well as free hydrogels in solution. Gelation of 0.60% alginate cores was also achieved in a four inlets device using CLEX. The latter gelation method is somewhat more intricate than the former, as it involves an extra phase which complicates the double emulsion synthesis. However, CLEX provides a non-acidic environment which is favorable for encapsulation of microorganisms that are sensitive to pH changes. Additionally, the four inlets device introduces the possibility of on-chip mixing of cargo for encapsulation experiments.

Pseudomonas Putida and *Chlamydomonas reinhardtii* were encapsulated in double emulsions synthesized in microfluidic devices and immobilized on PDMS microarrays. Double emulsion cores consisting of either 20% PEG, 0.15% alginate, or 0.60% alginate were tested as

encapsulation media for optimization of a cell-friendly microenvironment. Neither PEG nor 0.60% alginate cores provided healthy environments for normal cellular activity and proliferation; PEG was found to be detrimental to bacterial viability, and cores consisting of 0.60% alginate inhibited both bacterial and algal cell motility and proliferation, probably due to high viscosity. On the other hand, bacterial colonies grew steadily when encapsulated in 0.15% alginate cores. The double emulsions showed stability with regards to coalescence, temperature variations and shear. However, due to osmotic pressure differences between the double emulsion cores and carrier fluid, the double emulsions containing growing bacterial colonies burst around four hours after encapsulation. It is likely that this issue can be overcome by increasing the amount of sucrose present in the carrier fluid, however, a precise determination of the required amount of sucrose would necessitate accurate screening tests or osmometric measurements for the given system. Nevertheless, proliferation in 0.15% alginate cores proved that the double emulsions and microarray presented in this work represent a suitable platform for microbial encapsulation and growth analysis, if the osmotic instability issue is resolved.

The synthesis of double emulsions of varying sizes and different amounts of cores was also demonstrated. This was achieved by adjusting flow rates and fluid viscosities, although with some variation and uncertainty. A fine-tuned system relies mainly on the alignment of the device, the microchannel surface treatment and the tubing of the syringe pump system, which might vary from experiment to experiment. Generally, the double emulsions synthesized in this work varied from 50 µm and 100 µm in outer diameter and 20 µm and 80 µm in inner diameter, which are suitable sizes for cell encapsulation.

A complete double emulsion platform for cell encapsulation and analysis is contingent on resolving the osmotic pressure instability issue. For future work, an osmometer should be available for each specific experiment. If an osmometer is inaccessible, thorough screening tests should be conducted to determine the amount of sucrose necessary for all double emulsion compositions. Once a protocol for stable double emulsions is established, further cell encapsulation and analysis of cellular processes can be performed. Of particular interest is the application of the four inlets device for on-chip mixing of different types of cargo. By introducing donor and recipient cells separately through the two inner aqueous phase inlets,

cellular processes such as bacterial conjugation can be studied. Another interesting topic for study is the use of CLEX in the four inlets device for a non-acidic encapsulation of biological material in hydrogels, which remains to be tested. Furthermore, CLEX offers the opportunity of well-timed gelation by variation of chelates and exchange ions, which also could be investigated in the four inlets device. Finally, for enhanced single-cell encapsulation rates, a downstream sorting system should be devised to separate empty double emulsions from the population. SSAW could be applied for this purpose, and should be integrated in future setups.

Appendix A

Acronyms

WOW Water-in-oil-in-water

CaEDTA Ca-Ethylenediaminetetraacetic acid

CLEX Competitive Ligand Exchange crosslinking

ZnEDDA Zn-Ethylenediamine diacetate

PFPE Perfluoropolyether

PEG Polyethylene glycol

HFE7500 HFE7500 3M^{TM} Novec^{TM} Engineered Fluid

PVA Polyvinyl alcohol

rpm Revolutions per minute

PDMS Polydimethylsiloxane

SMaL Soft Materials Laboratory

EPFL École Polytechnique Fédérale de Lausanne

kDa Kilodalton

Mq-water Milli-Q water, ultra pure water from Millipore Corporation

GFP Green fluorescent protein

FS Forward scatter

SS Side scatter

SSAW Standing surface acoustic wave

Appendix B

Flow cytometry

Flow cytometers are high-throughput, single particle-resolution instruments used for quantitative particle analysis[93]. In a modern flow cytometer, particles in suspension pass individually through a laser beam at rates of some 1000 particles/s. Fluorescence signals and the extent of side- and forward scattered light are measured by appropriate detectors, permitting a display of the number of particles possessing a certain quantitative property. The forward scattered (FS) light is related to the particle size, while side-scatter (SS) reveals information on the particle granularity. Fluorescence signals may be used to detect a variety of biomarkers present in the sample. WOW double emulsions have been used as compartments for flow cytometry with reported success, and have been suggested as a suitable platform for directed evolution, as their uniformity provides a high screening accuracy[94][46].

Here, double emulsions were analyzed in a flow cytometer (Gallios, Beckman Coulter) using 488 nm (FS, SS) and 561 nm (fluorescence excitation) lasers and a 525 nm (BP 40) detection filter. The double emulsions consisted of cores containing 0.15% alginate dissolved in LB with HFE7500 oil shells and were suspended in 9.2% PVA with 100 gL^{-1} sucrose. The emulsions were stabilized by surfactants (2% (w/w)) in the oil phase. The sample was diluted 50/50 with Mq-water containing 100 gL^{-1} sucrose before analysis to reduce the viscosity without destabilizing the droplets. Additionally, *Pseudomonas Putida* were encapsulated and GFP expression induced by the addition of 0.5 mM m-Toluic acid to explore the possibility of cell detection within the double emulsions.

The results from the flow cytometry data analysis are presented in Figure B.1. The ungated

SS vs. FS plot (top left) reveals a population of double emulsions with a spreading in both size and granularity. The extent of this distribution is unknown, as no control sample with particles of a known size was tested for comparison. Particle size variation seems close to normally distributed in the accompanying histogram (top right). The fluorescence detection (bottom right) shows an increase in fluorescence emission for increased particle size. It is possible that this is due to higher cell content, which is additionally supported by the increased granularity for larger droplets. However, LB medium was found to exhibit autofluorescence in a range of about 500 nm - 600 nm, which overlaps with GFP emission spectra[95]. It is thus likely that the increase in fluorescence is mostly due to the fact that larger droplets have larger cores, and thus emit higher levels of autofluorescence. The fluorescence histogram (bottom left) shows the variation in fluorescence, which is a little less than a tenfold stronger for the most emitting particles than the least emitting ones.

A more detailed analysis would require several controls to quantify double emulsion size and dispersity as well as to separate fluorescence emission from GFP expressing bacteria and LB autofluorescence. However, these results prove that the double emulsions produced in this work are able to withstand the shear induced in a flow cytometer and therefore provide a flow cytometry friendly platform for single-cell analysis.

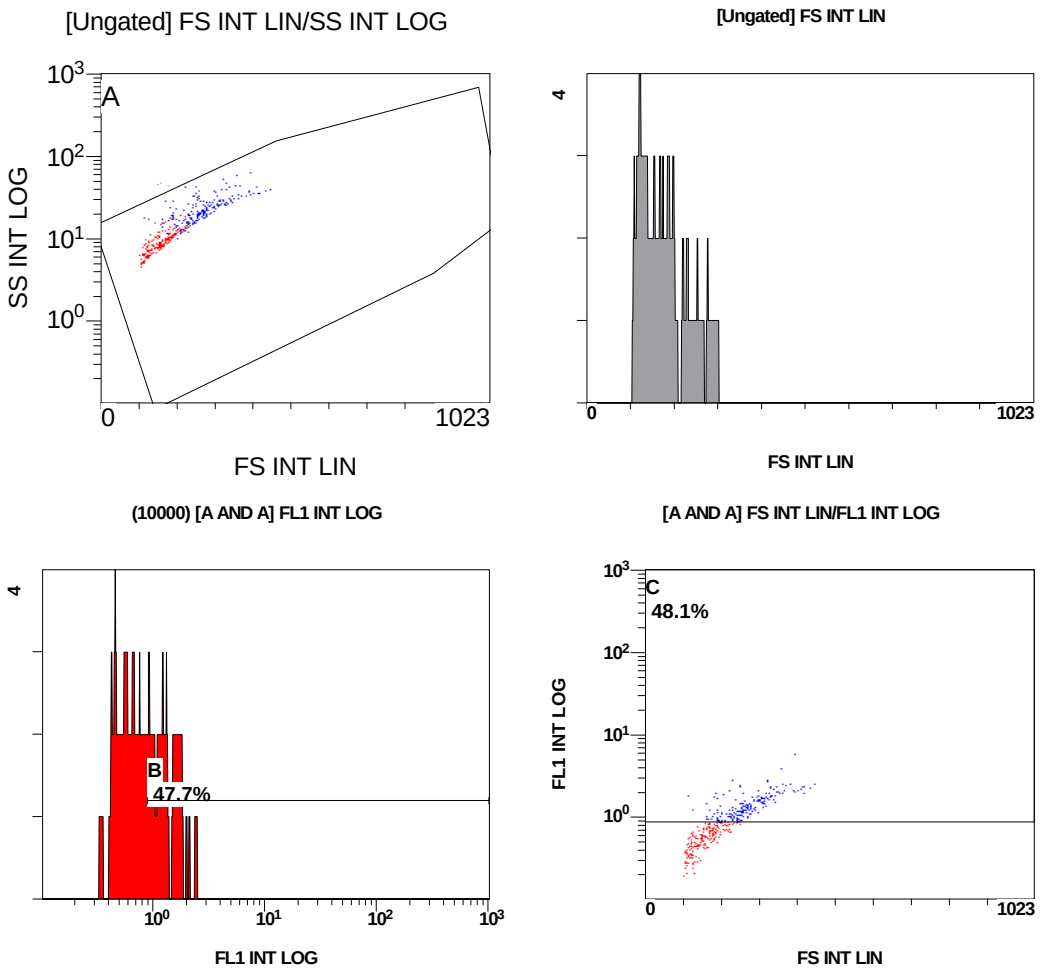

Figure B.1: Statistical data from the flow cytometer analysis of double emulsions containing GFP expressing bacteria and autofluorescent cores. Top left: A SS vs. FS plot reveals information about particle size and granularity. Top right: Histogram displaying the variation in particle size. Bottom left: Histogram displaying the variation in emitted fluorescence. Bottom right: A fluorescence vs. FS plot shows the relationship between the emitted fluorescence and particle size. A more detailed discussion of the data is found in the text.

Bibliography

[1] Byron F Brehm-stecher and Eric A Johnson. Single-Cell Microbiology: Tools, Technologies, and Applications. *Microbiology and Molecular Biology Reviews*, 68(3):538–559, 2004.

[2] WHO: Antimicrobial resistance. http://www.who.int/mediacentre/factsheets/fs194/en/, 2015.

[3] A Giedraitiene, A Vitkauskiene, R Naginiene, and A Pavilonis. Antibiotic resistance mechanisms of clinically important bacteria. *Medicina (Kaunas)*, 47(3):137–146, 2011.

[4] Tiago R D Costa, Catarina Felisberto-Rodrigues, Amit Meir, Marie S Prevost, Adam Redzej, Martina Trokter, and Gabriel Waksman. Secretion systems in Gram-negative bacteria: structural and mechanistic insights. *Nat Rev Micro*, 13(6):343–359, 2015.

[5] David J. Collins, Adrian Neild, Andrew DeMello, Ai-Qun Liu, and Ye Ai. The Poisson distribution and beyond: methods for microfluidic droplet production and single cell encapsulation. *Lab Chip*, pages 3439–3459, 2015.

[6] Toshiya Takeda, Takanori Kitagawa, Yoshikuni Takeuchi, Minoru Seki, and Shintaro Furusaki. Metabolic responses of plant cell culture to hydrodynamic stress. *The Canadian Journal of Chemical Engineering*, 76(2):267–275, 1998.

[7] Luca Gasperini, João F Mano, and Rui L Reis. Natural polymers for the microencapsulation of cells. *Journal of the Royal Society, Interface / the Royal Society*, 11(100):20140817, 2014.

[8] Christophe F. Meunier, Philippe Dandoy, and Bao Lian Su. Encapsulation of cells within silica matrixes: Towards a new advance in the conception of living hybrid materials. *Journal of Colloid and Interface Science*, 342(2):211–224, 2010.

[9] Makhlouf Amoura, Nadine Nassif, Cécile Roux, Jacques Livage, and Thibaud Coradin. Sol-gel encapsulation of cells is not limited to silica: long-term viability of bacteria in alumina matrices. *Chemical communications (Cambridge, England)*, (39):4015–4017, 2007.

[10] Alberto Diaspro, Daniela Silvano, Silke Krol, Ornella Cavalleri, and Alessandra Gliozzi. Single living cell encapsulation in nano-organized polyelectrolyte shells. *Langmuir*, 18(13):5047–5050, 2002.

[11] Samin Akbari and Tohid Pirbodaghi. Microfluidic encapsulation of cells in alginate particles via an improved internal gelation approach. *Microfluidics and Nanofluidics*, pages 1–5, 2013.

[12] Shinji Sugiura, Tatsuya Oda, Yasuhiko Izumida, Yasuyuki Aoyagi, Mitsuo Satake, Atsushi Ochiai, Nobuhiro Ohkohchi, and Mitsutoshi Nakajima. Size control of calcium alginate beads containing living cells using micro-nozzle array. *Biomaterials*, 26(16):3327–3331, 2005.

[13] Kuen Yong Lee and David J. Mooney. Alginate: Properties and biomedical applications. *Progress in Polymer Science (Oxford)*, 37(1):106–126, 2012.

[14] Sarah Köster, Francesco E Angilè, Honey Duan, Jeremy J Agresti, Anton Wintner, Christian Schmitz, Amy C Rowat, Christoph a Merten, Dario Pisignano, Andrew D Griffiths, and David a Weitz. Drop-based microfluidic devices for encapsulation of single cells. *Lab on a chip*, 8(7):1110–1115, 2008.

[15] Jean-Christophe Baret. Surfactants in droplet-based microfluidics. *Lab on a Chip*, (12), 2012.

[16] Lisa R Volpatti and Ali K Yetisen. Commercialization of microfluidic devices. *Trends in Biotechnology*, 32(7):347–350, 2014.

[17] Mohammad Tarameshlou, Seyed Hassan Jafari, Iraj Rezaeian, and Hossein Ali Khonakdar. A Microfluidic Approach to Synthesize Monodisperse Poly (2-Hydroxyethyl Methacrylate) Based Spherical Microgels via Water in Water Emulsion Technique. *International Journal of Polymeric Materials and Polymeric Biomaterials*, (63):884–890, 2014.

[18] Jonathan H. Tsui, Woohyuk Lee, Suzie H. Pun, Jungkyu Kim, and Deok Ho Kim. Microfluidics-assisted in vitro drug screening and carrier production. *Advanced Drug Delivery Reviews*, 65(11-12):1575–1588, 2013.

[19] Sissel Juul, Christine J F Nielsen, Rodrigo Labouriau, Amit Roy, Cinzia Tesauro, Pia W Jensen, Charlotte Harmsen, Emil L Kristoffersen, Ya-ling Chiu, Paola Fiorani, Janet Coxsingh, David Tordrup, Jørn Koch, Alessandro Desideri, Stephane Picot, Eskild Petersen, Kam W Leong, Ping Ho, Magnus Stougaard, Birgitta R Knudsen, and De Lyon. A Droplet Microfluidics Platform for Highly Sensitive and Quantitative Detection of Malaria Causing Plasmodium Parasites Based on Enzyme Activity Measurement. 2012.

[20] Balint Kintses, Christopher Hein, Mark F. Mohamed, Martin Fischlechner, Fabienne Courtois, Céline Lainé, and Florian Hollfelder. Picoliter cell lysate assays in microfluidic droplet compartments for directed enzyme evolution. *Chemistry and Biology*, 19(8):1001–1009, 2012.

[21] Pierre-Yves Colin, Balint Kintses, Fabrice Gielen, Charlotte M Miton, Gerhard Fischer, Mark F Mohamed, Marko Hyvönen, Diego P Morgavi, Dick B Janssen, and Florian Hollfelder. Ultrahigh-throughput discovery of promiscuous enzymes by picodroplet functional metagenomics. *Nature communications*, 6:10008, 2015.

[22] Maximilian Weitz, Andrea Muckl, Korbinian Kapsner, Ronja Berg, Andrea Meyer, and Friedrich C. Simmel. Communication and computation by bacteria compartmentalized within microemulsion droplets. *Journal of the American Chemical Society*, 136(1):72–75, 2014.

[23] Hamad A. Al-Hajry, Salha A. Al-Maskry, Latifa M. Al-Kharousi, Osman El-Mardi, Walid H. Shayya, and M. F A Goosen. Electrostatic encapsulation and growth of plant cell cultures in alginate. *Biotechnology Progress*, 15(4):768–774, 1999.

[24] Verica Manojlovic, Jasna Djonlagic, Bojana Obradovic, Viktor Nedovic, and Branko Bugarski. Investigations of cell immobilization in alginate: Rheological and electrostatic extrusion studies. *Journal of Chemical Technology and Biotechnology*, 81(4):505–510, 2006.

[25] Chang-Hyung Choi, Huanan Wang, Hyomin Lee, June Hwan Kim, Liyuan Zhang, Angelo Mao, David J. Mooney, and David A. Weitz. One-step generation of cell-laden mi-

crogels using double emulsion drops with a sacrificial ultra-thin oil shell. *Lab Chip*, 16:1549–1555, 2016.

[26] Ying Zhang, Yi Ping Ho, Ya Ling Chiu, Hon Fai Chan, Ben Chlebina, Tom Schuhmann, Lingchong You, and Kam W. Leong. A programmable microenvironment for cellular studies via microfluidics-generated double emulsions. *Biomaterials*, 34(19):4564–4572, 2013.

[27] Fu-Che Chang and Yu-Chuan Su. Controlled double emulsification utilizing 3D PDMS microchannels. *Journal of Micromechanics and Microengineering*, 18(6), 2008.

[28] Shih-Hao Huang, Wei-Heong Tan, Fan-Gang Tseng, and Shoji Takeuchi. A monolithically three-dimensional flow-focusing device for formation of single/double emulsions in closed/open microfluidic systems. *Journal of Micromechanics and Microengineering*, 16(11), 2006.

[29] N Wu, J G Oakeshott, C J Easton, T S Peat, R Surjadi, and Y Zhu. A double-emulsion microfluidic platform for in vitro green fluorescent protein expression. *Journal of Micromechanics and Microengineering*, 21(5):054032, 2011.

[30] Connie B. Chang, James N. Wilking, Shin Hyun Kim, Ho Cheung Shum, and David A. Weitz. Monodisperse Emulsion Drop Microenvironments for Bacterial Biofilm Growth. *Small*, 11(32):3954–3961, 2015.

[31] Tae Yong Lee, PraveenKumar Ramasamy, You-Kwan Oh, Kyubock Lee, and Shin-Hyun Kim. Alginate Microgels Created by Selective Coalescence between Core Drops Paired by Ultrathin Shell. *J. Mater. Chem. B*, 4(19):3232–3238, 2016.

[32] Frank M White. *Fluid Mechanics*. McGraw-Hill, New York, NY, 6th edition, 2009.

[33] Henrik Bruus. *Theoretical Microfluidics*. Oxford {Master} {Series} in {Condensed} {Matter} {Physics}. Oxford University Press, Great Clarendon Street, Oxford OX2 6DP, 1. edition, 2008.

[34] L R Arriaga, Esther Amstad, and D A Weitz. Scalable single-step microfluidic production of single-core double emulsions with ultra-thin shells. *Lab on a Chip*, 15:3335–3340, 2015.

[35] Preben C Mørk. *Overflate og kolloidkjemi*. Institutt for kjemisk prosessteknologi, Fakultet for naturvitenskap og teknologi, NTNU, Trondheim, 8. edition, 2004.

[36] D H Everett. Manual of Symbols and Terminology for Physiochemical Quantities and Units, Appendix II, Part 1, 1971.

[37] P C Hemmer. *Termisk fysikk*. Tapir akademisk forlag, 2. edition, 2002.

[38] Ole G Mouritsen. *Life - as a matter of fat. The emerging science of lipidomics*. Springer, 1st edition, 2005.

[39] C Holtze, A C Rowat, J J Agresti, J B Hutchison, F E Angile, C H J Schmitz, S Koster, H Duan, K J Humphry, R A Scanga, J S Johnson, D Pisignano, D a Weitz, F E Angilè, C H J Schmitz, S Köster, H Duan, K J Humphry, R A Scanga, J S Johnson, D Pisignano, and D a Weitz. Biocompatible surfactants for water-in-fluorocarbon emulsions. *Lab on a Chip*, 8(10):1632–1639, 2008.

[40] Ya-ling Chiu, Hon Fai Chan, Kyle K. L. Phua, Ying Zhang, Sissel Juul, Birgitta Ruth Knudsen, Yi-Ping Ho, and Kam W. Leong. Synthesis of Fluorosurfactants for Emulsion-Based Biological Applications. *ACS Nano*, 8(4):3913–3920, 2014.

[41] Olaf Wagner, Julian Thiele, Marie Weinhart, Linas Mazutis, David A Weitz, Wilhelm T S Huck, and Rainer Haag. Biocompatible fluorinated polyglycerols for droplet microfluidics as an alternative to PEG-based copolymer surfactants. *Lab on a chip*, 16(1):65–9, 2016.

[42] Suk Kyu Han and Byung Hak Jhun. Effect of additives on the cloud point of polyethylene glycols. *Archives of Pharmacal Research*, 7(1):1–9, 1984.

[43] Demetrios T Papageorgiou. On the breakup of viscous liquid threads. *Physics of Fluids*, 7(7):1529–1544, 1995.

[44] S Tomotika. On the Instability of a Cylindrical Thread of a Viscous Liquid Surrounded by Another Viscous Fluid. *The Royal Society*, 150(870), 1935.

[45] John R Richards, Abraham M Lenhoff, and Antony N Beris. Dynamic breakup of liquid–liquid jets. *Physics of Fluids*, 6:2640, 1994.

[46] Jing Yan, Wolfgang-Andreas C Bauer, Martin Fischlechner, Florian Hollfelder, Clemens F Kaminski, and Wilhelm T S Huck. Monodisperse Water-in-Oil-in-Water (W/O/W) Double Emulsion Droplets as Uniform Compartments for High-Throughput Analysis via Flow Cytometry. *Micromachines*, (4):402–413, 2013.

[47] A S Utada, E Lorenceau, D R Link, P D Kaplan, H A Stone, and D A Weitz. Monodisperse Double Emulsions Generated from a Microcapillary Device. *Science*, 308(5721):537–541, apr 2005.

[48] Assaf Rotem, Adam R Abate, Andrew S Utada, Volkert Van Steijn, and David A Weitz. Drop formation in non-planar microfluidic devices. *Lab on a Chip*, 12:4263–4268, 2012.

[49] 3M. 3M™ Novec™ 7500 Engineered Fluid, 2008.

[50] Joseph Kestin, Mordechai Sokolov, and William A. Wakeham. Viscosity of liquid water in the range minus 8 to 150 degrees celsius. *Journal of Physical and Chemical Reference Data*, 7(3):941, 1978.

[51] Esther Amstad, Shin-Hyun Kim, and David A Weitz. Photo- and Thermoresponsive Polymersomes for Triggered Release. *Angewandte Chemie International Edition*, 51(50):12499–12503, 2012.

[52] Ana Cristina de Souza, Cynthia Ditchfield, and Carmen Cecilia Tadini. Biodegradable Films Based on Biopolymers for Food Industries. In Maria Laura Passos and Claudio P Ribeiro, editors, *Innovation in Food Engineering: New Techniques and Products*, chapter 17, pages 520–521. CRC Press, 1st edition, 2009.

[53] C S Cox. Bacterial survival in suspension in polyethylene glycol solutions. *Journal of general microbiology*, 45(1966):275–281, 1966.

[54] J. Chirife, L. Herszage, A. Joseph, J. P. Bozzini, N. Leardini, and E. S. Kohn. In vitro antibacterial activity of concentrated polyethylene glycol 400 solutions. *Antimicrobial Agents and Chemotherapy*, 24(3):409–412, 1983.

[55] U. Ambrose, K. Middleton, and D. Seal. In vitro studies of water activity and bacterial growth inhibition of sucrose-polyethylene glycol 400-hydrogen peroxide and xylose-polyethylene glycol 400-hydrogen peroxide pastes used to treat infected wounds. *Antimicrobial Agents and Chemotherapy*, 35(9):1799–1803, 1991.

[56] Bjørn E Christensen. *Compendium TBT4135 Biopolymers*. NOBIPOL, Department of Biotechnology, NTNU, 2015.

[57] Peter Gacesa. Alginates. *Carbohydrate Polymer*, 8:161–182, 1988.

[58] Stefanie Utech, Radivoje Prodanovic, Angelo S. Mao, Raluca Ostafe, David J. Mooney, and David A. Weitz. Microfluidic Generation of Monodisperse, Structurally Homogeneous Alginate Microgels for Cell Encapsulation and 3D Cell Culture. *Advanced Healthcare Materials*, 4(11):1628–1633, 2015.

[59] Armend G. Håti, David C. Bassett, Jonas M. Ribe, Pawel Sikorski, David A. Weitz, and Bjørn Torger Stokke. Simple, universal, cell and chip friendly method to gel alginate in microfluidic devices. *Submitted*, 2016.

[60] Lai Wah Chan, Huey Ying Lee, and Paul W S Heng. Mechanisms of external and internal gelation and their impact on the functions of alginate as a coat and delivery system. *Carbohydrate Polymers*, 63(2):176–187, 2006.

[61] Kurt Ingar Draget, Kjetill Ostgaard, and Olav Smidsrød. Alginate-based solid media for plant tissue culture. *Applied microbiology and Biotechnology*, 31:79–83, 1989.

[62] David C. Bassett, Armend G. Håti, Thor Bernt Melø, Bjørn Torger Stokke, and Pawel Sikorski. Competitive Ligand Exchange of Crosslinking Ions for Ionotropic Hydrogel Formation. *Under review*, 2016.

[63] Timothy A. Becker, Daryl R. Kipke, and Tedd Brandon. Calcium alginate gel: A biocompatible and mechanically stable polymer for endovascular embolization. *Journal of Biomedical Materials Research*, 54(1):76–86, 2001.

[64] K. E. Nelson, C. Weinel, I. T. Paulsen, R. J. Dodson, H. Hilbert, V. A P Martins dos Santos, D. E. Fouts, S. R. Gill, M. Pop, M. Holmes, L. Brinkac, M. Beanan, R. T. DeBoy, S. Daugherty, J. Kolonay, R. Madupu, W. Nelson, O. White, J. Peterson, H. Khouri, I. Hance, P. Chris Lee, E. Holtzapple, D. Scanlan, K. Tran, A. Moazzez, T. Utterback, M. Rizzo, K. Lee, D. Kosack, D. Moestl, H. Wedler, J. Lauber, D. Stjepandic, J. Hoheisel, M. Straetz, S. Heim, C. Kiewitz, J. Eisen, K. N. Timmis, A. D??sterh??ft, B. T??mmler, and C. M. Fraser. Complete genome sequence and comparative analysis of the metabolically versatile Pseudomonas putida KT2440. *Environmental Microbiology*, 4(12):799–808, 2002.

[65] J L Salisbury, M a Sanders, and L Harpst. Flagellar Root Contraction and Nuclear-Movement During Flagellar Regeneration in Chlamydomonas-Reinhardtii. *Journal of Cell Biology*, 105(4):1799–1805, 1987.

[66] C S Harwood, K Fosnaugh, and M Dispensa. Flagellation of Pseudomonas-Putida and Analysis of Its Motile Behavior. *Journal of Bacteriology*, 171(7):4063–4066, 1989.

[67] Eric Lauga and Thomas R Powers. The hydrodynamics of swimming microorganisms. *Reports on Progress in Physics*, 72(9):096601, 2009.

[68] Dong Qin, Younan Xia, and George M Whitesides. Soft lithography for micro- and nanoscale patterning. *Nature*, 5(3):491–502, 2010.

[69] Sindy K Y Tang and George M Whitesides. Chapter 2: Basic Microfluidic and Soft Lithographic Techniques. In *Optofluidics. {Fundamentals}, {Devices}, and {Applications}*, Biophotonics. McGraw-Hill, 1. edition, 2010.

[70] Ingrid Hoek, Febly Tho, and W Mike Arnold. Sodium hydroxide treatment of PDMS based microfluidic devices. *Lab on a Chip*, (10), 2010.

[71] Gymama Slaughter and Brian Stevens. A cost-effective two-step method for enhancing the hydrophilicity of PDMS surfaces. *BioChip Journal*, 8(1):28–34, 2014.

[72] Wolfgang-Andreas C Bauer, Martin Fischlechner, Chris Abell, and Wilhelm T S Huck. Hydrophilic PDMS microchannels for high-throughput formation of oil-in-water microdroplets and water-in-oil-in-water double emulsions. *Lab on a Chip*, 10:1814–1819, 2010.

[73] Ieong Wong and Chih-Ming Ho. Surface molecular property modifications for poly(dimethylsiloxane) (PDMS) based microfluidic devices. *Microfluid Nanofluidics*, 7(3):291–306, 2009.

[74] Roya Maboudian, W Robert Ashurst, and Carlo Carraro. Self-assembled monolayers as anti-stiction coatings for MEMS: characteristics and recent developments. *Sensors and Actuators*, 82:219–223, 1999.

[75] Product Specification - Trichloro(1H,1H,2H,2H-perfluorooctyl)silane, 2015.

[76] J. H. Miller. *Experiments in molecular genetics*. Cold Spring Harbor Laboratory, Cold Spring Harbor, New York, 1972.

[77] Culture Collection of Cryophilic Algae: TAP -Medium (Tris-Acetate-Phosphate). Technical report, Fraunhofer, 2014.

[78] Marie Pierre Krafft. Fluorocarbons and fluorinated amphiphiles in drug delivery and biomedical research. *Advanced Drug Delivery Reviews*, 47(2-3):209–228, 2001.

[79] Philipp Gruner, Birte Riechers, Benoît Semin, Jiseok Lim, Abigail Johnston, Kathleen Short, and Jean-Christophe Baret. Controlling Molecular Transport in Minimal Emulsions. *Nature Communications*, page in press, 2015.

[80] P. D. Scholes, A. G A Coombes, L. Illum, S. S. Daviz, M. Vert, and M. C. Davies. The preparation of sub-200 nm poly(lactide-co-glycolide) microspheres for site-specific drug delivery. *Journal of Controlled Release*, 25(1-2):145–153, 1993.

[81] John Sharpe and Sonja Wulff. Flow Cytometry Education Guide. *Dako Knowledge Center*, Education(Flow Cytometry):33–40, 2005.

[82] Ho Cheung Shum, Daeyeon Lee, Insun Yoon, Tom Kodger, and David A. Weitz. Double emulsion templated monodisperse phospholipid vesicles. *Langmuir*, 24(15):7651–7653, 2008.

[83] Chiara Martino, Tae Yong Lee, Shin Hyun Kim, and Andrew J. DeMello. Microfluidic generation of PEG-b-PLA polymersomes containing alginate-based core hydrogel. *Biomicrofluidics*, 9(2), 2015.

[84] Mark a. Reinsel, John J. Borkowski, and John T. Sears. Partition Coefficients for Acetic, Propionic, and Butyric Acids in a Crude Oil/Water System. *Journal of Chemical & Engineering Data*, 39(3):513–516, 1994.

[85] Samaneh Mashaghi and Antoine M. van Oijen. External control of reactions in microdroplets. *Scientific Reports*, 5:11837, 2015.

[86] Y V Griko. Energetics of Ca(2+)-EDTA interactions: calorimetric study. *Biophysical chemistry*, 79(2):117–27, 1999.

[87] Qiushui Chen, Stefanie Utech, Dong Chen, Radivoje M. Prodanovic, Jin-Ming Lin, and David A. Weitz. Controlled Assembly of Heterotypic cells in a Core-Shell Scaffold: Organ in a Droplet. *Lab Chip*, 16:1346–1349, 2016.

[88] Fumiki Yanagawa, Hirokazu Kaji, Yun Ho Jang, Hojae Bae, Du Yanan, Junji Fukuda, Hao Qi, and Ali Khademhosseini. Directed assembly of cell-laden microgels for building porous three-dimensional tissue constructs. *Journal of Biomedical Materials Research - Part A*, 97 A(1):93–102, 2011.

[89] Ahmad Ahsan Nawaz, Yuchao Chen, Nitesh Nama, Ruth Helmus Nissly, Liqiang Ren, Adem Ozcelik, Lin Wang, J. Philip McCoy, Stewart J. Levine, and Tony Jun Huang. Acoustofluidic Fluorescence Activated Cell Sorter. *Analytical Chemistry*, 87(24):12051–12058, 2015.

[90] Jean-Christophe Baret, Oliver J. Miller, Valerie Taly, Michaël Ryckelynck, Abdeslam El-Harrak, Lucas Frenz, Christian Rick, Michael L. Samuels, J. Brian Hutchison, Jeremy J. Agresti, Darren R. Link, David A. Weitz, and Andrew D. Griffiths. Fluorescence-activated droplet sorting (FADS): efficient microfluidic cell sorting based on enzymatic activity. *Lab on a chip*, 9(13):1850–8, 2009.

[91] B Alberts, A Johnson, and J Lewis. *Molecular Biology of the Cell*. Garland Science, 4th edition, 2002.

[92] Revathi Ananthakrishnan and Allen Ehrlicher. The forces behind cell movement. *International Journal of Biological Sciences*, 3(5):303–317, 2007.

[93] H M Davey and D B Kell. Flow cytometry and cell sorting of heterogeneous microbial populations: the importance of single-cell analyses. *Microbiological reviews*, 60(4):641–696, 1996.

[94] Shaun W Lim and Adam R Abate. Ultrahigh-throughput sorting of microfluidic drops with flow cytometry. *Lab on a chip*, 13(23):4563–72, 2013.

[95] G Patterson, R N Day, and D Piston. Fluorescent protein spectra. *Journal of cell science*, 114(Pt 5):837–838, 2001.